Energy Strategy Reviews 65 (2026) 102146

Contents lists available at ScienceDirect

Energy Strategy Reviews

journal homepage: www.elsevier.com/locate/esr

Transporting the future: A methodology and case study for pipeline imports of hydrogen derivatives to Germany

Natalia Pieton [a,b,*], Bastian Weissenburger [c,d], Lukas Karkossa [e], Marius Neuwirth [c], Martin Wietschel [c]

[a] Fraunhofer Research Institution for Energy Infrastructures and Geotechnologies IEG, Germany
[b] Karlsruhe Institute of Technology, Germany
[c] Fraunhofer Institute for Systems and Innovation Research ISI, Germany
[d] Chair of Energy Systems Analysis, Institute of Energy and Process Engineering, ETH Zürich, Switzerland
[e] Department of Wind and Energy Systems, Technical University of Denmark, Denmark

ARTICLE INFO

Handling Editor: Dr. Henrik Lund

Keywords:
Pipeline modelling
GIS
Energy imports
Hydrogen derivatives
Energy carriers
CO_2

ABSTRACT

Germany's energy transition will require large-scale imports of hydrogen and its derivatives from regions with high renewable energy potential. While pipeline-based imports of hydrogen and ship-based imports of hydrogen derivatives are widely discussed, pipeline imports of liquid derivatives remain underexplored. Existing cost analyses in the literature often neglect fluid-specific properties, pressure losses, and geography. This paper presents HyTROM+, a GIS-based methodology for determining optimal pipeline routes and the levelized cost of transport for hydrogen, CO_2, methanol, Fischer-Tropsch crude, and kerosene, considering both new and repurposed pipelines. The model integrates geographical factors, fluid mechanics, and techno-economic parameters to optimize the pipeline route and provide fluid-specific LCOT estimates. A case study demonstrates that it could be 10 times more cost-effective to transport liquid hydrogen derivatives via pipeline than hydrogen or CO_2, even across elevated Alpine terrain. A sensitivity analysis identifies pipeline capital expenses, infrastructure reuse, and the weighted average cost of capital as the main cost drivers. The results highlight the strategic importance of considering pipeline imports of liquid derivatives in infrastructure planning and suggest that repurposing existing oil and gas pipelines could offer substantial cost advantages.

1. Introduction

Germany is expected to still be reliant on energy imports in a climate-neutral future, as its domestic renewable energy (RE) potential will be insufficient to meet its long-term energy demand [1–3]. This is particularly relevant for sectors with high energy intensity and limited electrification potential, such as the steel, chemical, fertilizer, and refinery industries [4–6], long-term storage in power systems, and the international aviation and shipping sector [3].

1.1. The role of hydrogen derivatives in Germany's future energy system

Hydrogen and its derivatives are essential for becoming climate-neutral in hard-to-abate sectors [1]. Accordingly, ammonia and methanol are increasingly regarded as crucial hydrogen-derived energy carriers for value chains in chemical industry [2,3]. Together with synthetic diesel, they may play a growing role in maritime transport [2–4], supported by the FuelEU Maritime regulation [5], while Fischer Tropsch (FT) crude offers a promising substitute for fossil crude oil [7]. In parallel, the relevance of synthetic aviation fuels (eSAF) is expected to rise substantially as ReFuelEU Aviation quotas take effect from 2030 onwards [8]. At the same time, Germany currently assumes a leading role in shaping the emerging international hydrogen economy [9], and it remains a techno-economic and political question whether Europe should prioritize domestic production of hydrocarbons or rely on imports [10]. When produced from hydrogen and CO_2, both FT synthesis and the methanol-to-hydrocarbons (MtH) pathways are suitable options for generating climate-neutral hydrocarbons, such as fuels and high value chemicals (HVCs) [7]. CO_2 derived from Direct Air Capture (DAC) is particularly important, given the anticipated decline of point-source CO_2 as industrial processes become carbon-neutral and its potential to fully close carbon loops. RE largely determines DAC costs [11,12],

* Corresponding author. Fraunhofer Research Institution for Energy Infrastructures and Geotechnologies IEG, Germany.
E-mail address: Natalia.Pieton@ieg.fraunhofer.de (N. Pieton).

https://doi.org/10.1016/j.esr.2026.102146
Received 5 November 2025; Received in revised form 1 February 2026; Accepted 12 February 2026
Available online 6 April 2026
2211-467X/© 2026 The Authors. Published by Elsevier Ltd. This is an open access article under the CC BY license (http://creativecommons.org/licenses/by/4.0/).

creating a trade-off between sourcing CO_2 from regions with low-cost RE and transport expenses.

For sectors including the chemical industry, refineries, aviation, and shipping, the use of hydrogen in Germany requires the development of additional hydrogen and CO_2 transport and storage infrastructure to enable the production of hydrocarbons. This raises the question of whether these sectors will source hydrogen and CO_2 (green gases) or import hydrocarbons (intermediates) like methanol or FT crude, or even final products, such as fuels (e.g. kerosene, diesel, naphtha) or HVC (e.g. ethylene, propylene) (Fig. 1). To assess whether value chains in Germany should start from green gases or intermediates, a full cost assessment, including production, conversion, transport, and integration, is essential to identify the most cost-effective import option.

1.2. The role of transport costs and pipelines in hydrogen supply chains

To support decarbonization, Germany's hydrogen import strategy envisages imports of 45 to 90 TWh of hydrogen and its derivatives by 2030, representing approximately 50 to 70% of the anticipated domestic demand [13]. These volumes are expected to be produced in countries with abundant RE resources and subsequently exported to Germany. In this context, hydrogen transport costs are a critical factor in determining the competitiveness of import options [14]. Findings from the HYPAT project show that pipeline transport from Morocco or Türkiye could account for 18% to 52% of total supply costs at the German border for volumes between 10 and 100 TWh/yr [14]. These findings underline the strategic importance of transport in determining the total import costs and industrial value chain decisions. In addition to that, importing hydrogen by pipeline could be competitive with shipping liquid hydrogen over long distances (e.g. from Morocco) [14]. Where molecular hydrogen is needed at the point of use, the literature [15,16] indicates that importing hydrogen directly is generally more feasible than importing and reconverting derivatives.

Pipelines are more economical than road and rail for large-scale transport of hydrogen [17], CO_2 [18,19], methanol [20,21], and oil [22], while shipping is more competitive for global routes and smaller volumes (see Fig. 7 in Ref. [23]). Pipelines can also foster strategic interdependence and partnership between countries [14].

Recent studies have compared importing hydrogen derivatives, such as methanol, ammonia or FT liquids, by ship with transporting gaseous hydrogen by pipeline [14,24–27], but do not consider transporting derivatives by pipeline. The pipeline transport of derivatives at scale may offer cost and infrastructure benefits, but remains underexplored in current research [28,29]. In the context of climate change and the global energy transition, oil and natural gas (NG) demand are projected to peak before 2030 and then decline by up to 75% by 2050 in a net-zero scenario [30]. This is likely to result in significant spare capacity in existing oil and NG pipelines. Repurposing these pipelines for alternative uses can be far more cost-effective than building new infrastructure or decommissioning. It is thus essential to include existing infrastructure when calculating transport costs.

1.3. Research gaps in modelling pipeline transport of hydrogen derivatives

A major research gap concerns the comprehensive assessment of transporting hydrogen derivatives by pipeline [28,29]. Cost comparisons of import options are incomplete if they do not account for fluid properties, geography, and the role of pumps and compressors. A comparison of hydrogen, CO_2, FT crude, methanol, and kerosene is needed, as these fluids differ in their density, viscosity, and pressure levels required. As demonstrated by fossil fuel logistics, fluids that are liquid under ambient conditions generally exhibit lower transport costs than gaseous carriers: Liquids have higher viscosity and energy density than gases, which results in greater friction- and elevation losses and therefore higher pumping costs [31,32]. In contrast, gases require higher operating pressures to increase their energy density, which increases pipeline material needs and overall transport costs [33].

Geographical factors such as slope, land use, and population density have a significant impact on pipeline routing and the associated transport costs. To date, GIS-based models have been successfully applied to fossil fuel pipelines [34,35]. More recently, Weiβenburger et al. [36] developed the Hydrogen Transport Route Optimization Model (HyTROM) as a solution for GIS-based hydrogen pipeline routing. It leverages georeferenced data and applies Least Cost Path Analysis via Dijkstra's algorithm to identify the optimal route. However, comparable modelling approaches for hydrogen derivatives like methanol or FT crude are still missing [28].

1.4. Research question and paper structure

To enable robust and comparative assessments of pipeline costs for different fluids, enhanced modelling approaches are required. These should integrate a wider range of fluids, account for pressure-dependent cost factors, and reflect the influence of geography on routing decisions. This leads to the following central research questions:

How do elevation and other geospatial and technical parameters influence the LCOT of pipeline transport for hydrogen, CO_2, FT crude, methanol, and kerosene, and what are the key cost drivers specific to each fluid type?

To answer these questions, we develop a dedicated LCOT-estimation framework for liquid and gas pipelines by integrating the Dijkstra shortest-path algorithm that accounts for fluid-specific physical properties, economic factors, and GIS information. The framework's applicability is demonstrated through a case study assessing pipeline transport for hydrogen and CO_2 as raw materials for e-fuel production and for FT crude and methanol as intermediates. Kerosene is included as the final product and as a representative long-chain hydrocarbon due to its projected importance in climate-neutral aviation [2,8].

Chapter 2 introduces the extended model framework HyTROM+, outlining the methodological advancements made to the original HyTROM model. These include the integration of pressure-dependent and fluid-specific techno-economic parameters into the routing algorithm. Chapter 3 presents a case study applying HyTROM+ to the Transalpine Pipeline (TAL) corridor between Trieste and Karlsruhe across the Alpine region. The case study demonstrates the model's applicability and how elevation affects the optimal route and LCOT for the considered fluids. It also includes a sensitivity analysis to identify the most influential techno-economic parameters. Chapter 4 summarizes the key findings and discusses methodological limitations. Chapter 5 concludes the study, interprets the results in the context of national energy strategies, and provides recommendations for future research and policy development. Additional information is provided in the **Supplementary data** and the **Appendix**.



Fig. 1. Green hydrogen-based supply chain for production of fuels and high value chemicals (HVC). Own overview.

2. Model framework: HyTROM+

The Python-based HyTROM+ tool is used to analyse optimal pipeline transport routes, pressure losses and the associated LCOT for gaseous and liquid fluids. These include hydrogen, liquefied CO_2, methanol, FT crude, and kerosene (kero). Fig. 2 outlines the model framework of HyTROM+, structured by data input, processing, and output. These components are described in more detail in the subchapters 2.2-2.4. Prior to that, subchapter 2.1 briefly outlines the key enhancements made to the original HyTROM model and explains why this was chosen as the underlying methodology.

2.1. Profound extensions to HyTROM

The Hydrogen Transport Route Optimization Model (HyTROM) was originally developed to identify optimal hydrogen pipeline routes using GIS-based data (land use, slope, population density, sea depth, pipeline corridors) and the Dijkstra algorithm [36]. HyTROM provides a robust framework for the assessment of pipeline imports due to the comprehensive GIS-based dataset and high resolution of a 6.5 km × 6.5 km tile size based on Franke et al. [37]. This tile size enables sufficiently accurate and rapid route optimization, while integrating the efficient Dijkstra algorithm further reduces the computational effort involved. Dijkstra's algorithm reliably identifies least-cost paths in graphs with non-negative edge weights, making it well-suited for GIS-based pipeline routing [38,39].

The extended version, HyTROM+, supports additional fluids including CO_2, methanol, FT crude, and kerosene. It features refined input, processing, and output modules. Inputs now include techno-economic parameters for pipelines, pumps, and compressors, along with fluid-specific properties such as density, viscosity, and pressure requirements. The updated model calculates LCOT for both new and repurposed pipelines. Processing involves initialization with parameters like diameter, mass flow rate, and pump spacing. Outputs include elevation profiles, pressure loss metrics, total pumping capacity, and LCOT values per route and fluid, in addition to a detailed cost breakdown per fluid.

2.2. Data input

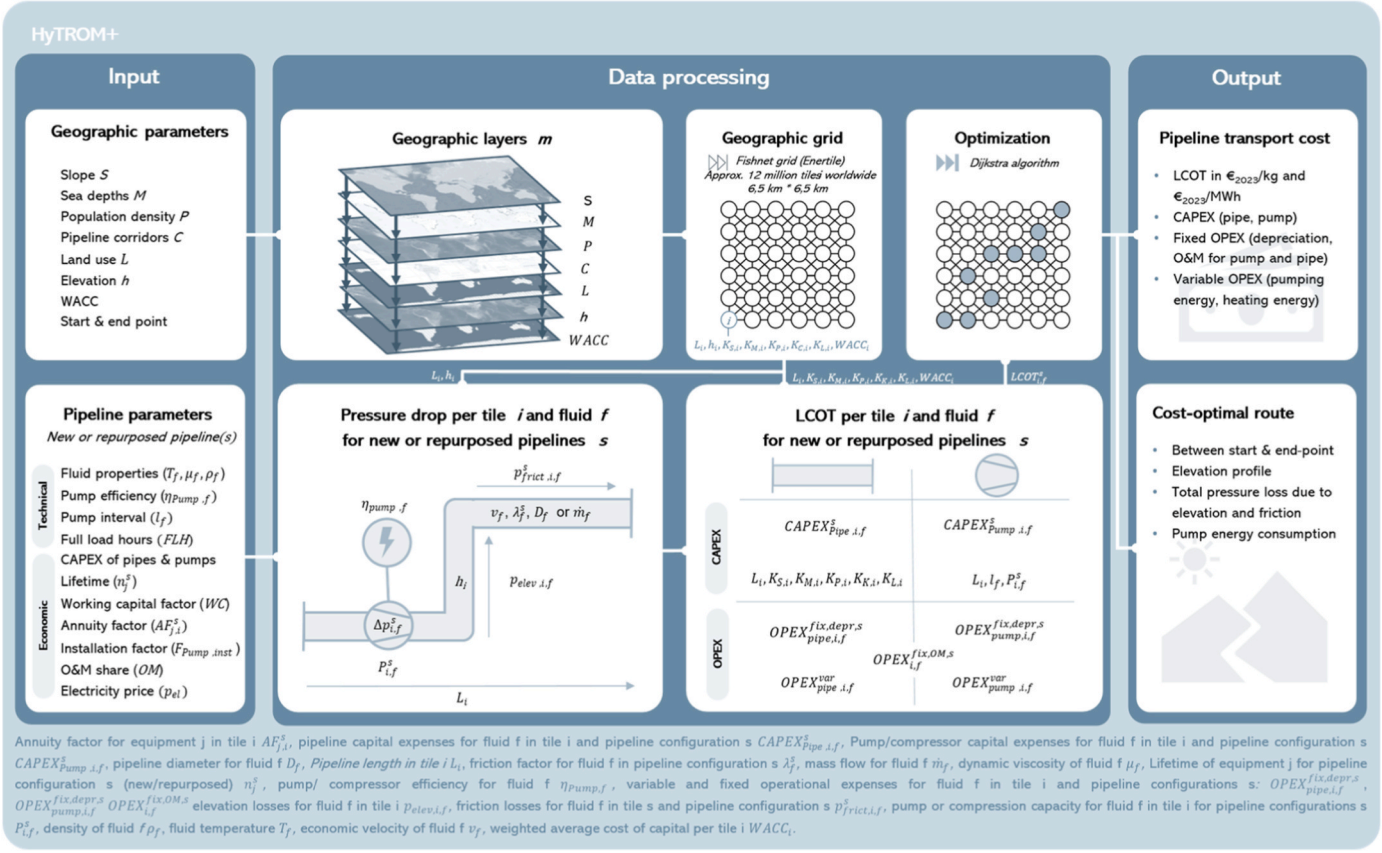
The input parameters are categorized as follows:

(1) **Geographical factors**, which account for routing constraints and the presence of existing pipeline infrastructure (distance, elevation, slope, land-use, population density, sea depth, pipeline corridor, weighted average cost of capital (WACC)).
(2) **Technical pipeline parameters**, used to determine economical diameters, pressure losses and pumping or compression capacities (phase, temperature, pressure level, viscosity, heating value, heat capacity, economic velocity, pipeline roughness, etc.).
(3) **Economic pipeline parameters**, which are used to estimate the resulting route and LCOT (fluid-specific pipeline and pump capital expenses (CAPEX) and lifetimes, pipeline factor, pump elevation factor, working capital share, operation and maintenance share, full-load hours (FLH), electricity price).

Detailed techno-economic data on the pipeline transport of different fluids remain limited [28]. An overview of the parameter values is provided in **Appendix B.2**.

2.3. Data processing

The input data are processed in four steps to generate model outputs in terms of the optimal transport route and the LCOT.



Annuity factor for equipment j in tile i $AF^s_{j,i}$, pipeline capital expenses for fluid f in tile i and pipeline configuration s $CAPEX^s_{Pipe\ i,f}$, Pump/compressor capital expenses for fluid f in tile i and pipeline configuration s $CAPEX^s_{Pump\ i,f}$, pipeline diameter for fluid f D_f, *Pipeline length in tile i* L_i, friction factor for fluid f in pipeline configuration s λ^s_f, mass flow for fluid f $\dot{m}_f$, dynamic viscosity of fluid f μ_f, Lifetime of equipment j for pipeline configuration s (new/repurposed) n^s_j, pump/ compressor efficiency for fluid f $\eta_{Pump,f}$, variable and fixed operational expenses for fluid f in tile i and pipeline configurations s: $OPEX^{fix,depr,s}_{pipe,i,f}$, $OPEX^{fix,depr,s}_{pump,i,f}$ $OPEX^{fix,OM,s}_{i,f}$ elevation losses for fluid f in tile i $p_{elev,i,f}$, friction losses for fluid f in tile s and pipeline configuration s $p^s_{frict,i,f}$, pump or compression capacity for fluid f in tile i for pipeline configurations s $P^s_{i,f}$, density of fluid f ρ_f, fluid temperature T_f, economic velocity of fluid f v_f, weighted average cost of capital per tile i $WACC_i$.

Fig. 2. Model framework: HyTROM+, adapted from Ref. [36].

Step 1: Model initialization. Parameters such as the start and end points, pipeline diameter or mass flow rate, and the corresponding fluid-specific pump intervals are defined exogenously. Furthermore, the pipeline configuration is selected as either new or repurposed for the entire route modelled. The region under consideration (e.g. a state, country, or continent) is divided into tiles of 6.5 km × 6.5 km, and its spatial extent must be large enough to fully contain both the defined start and end point.

Step 2: Pressure loss calculation per tile. The pressure loss is calculated for each tile in the region based on the fluid properties and technical pipeline parameters.

Step 3: LCOT calculation per tile. The LCOT is determined for each tile using the calculated pressure loss and associated economic parameters.

Step 4: Route optimization along tiles. The tile-specific LCOT values are assigned as weights to the edges connecting the tiles. The optimal transport route with the lowest cumulative edge weights is then identified using Dijkstra's algorithm, and the corresponding total LCOT is calculated.

The definition of diameter, mass flow, and pump intervals in the model initialization, the selection of newly constructed or repurposed pipelines, the pressure losses and LCOT calculation per tile, and the assignment of LCOT values to tile edges represent profound extensions to the original HyTROM model. Each of these steps is described in more detail in **Appendix B.3**.

2.4. Output

The main outputs of the model are the routing of each pipeline, pressure losses, and the resulting LCOT for hydrogen, CO_2, methanol, FT crude, and kerosene. For each fluid, the total pipeline distance is presented as an absolute value. Maps illustrate the general routing, highlighting the countries crossed, as well as regions with high population density, diverse land use, slopes, and elevation. Additionally, the elevation profile is included as a new feature of the model. HyTROM+ provides detailed information on pipeline pressure losses for each fluid, including friction losses, elevation losses, and elevation gains. This information allows us to determine the necessary pump capacity for each fluid and route. The total LCOT between the start and end points is provided for each fluid. A detailed cost breakdown is available, outlining specific cost components such as depreciation for pipelines and pumps, operational and maintenance costs (O&M), pumping energy, and heating costs.

3. Case study: importing hydrogen derivatives from Trieste to Karlsruhe

To demonstrate the model's functionality and assess the impact of elevation on pressure management and LCOT, a case study was conducted for transport through a 20-inch pipeline across the Alpine region. This corridor was selected due to its relevance as a potential import route for hydrogen [40], its potentially high elevation profile of up to 2500 m and its comparability with the existing TAL pipeline for oil transmission from Italy to Austria and Germany [41]. We assumed a 20-inch pipeline, as this is large enough to carry a meaningful share of hydrogen imports while avoiding unrealistic oversizing for liquid carriers. The mountainous terrain of the region is particularly relevant, as elevation can significantly affect pumping requirements and transport costs, especially for liquids. Therefore, the selected route serves as a stress test for the model rather than as a representative case for general LCOT estimations. Further case studies will be required to estimate LCOT under different geographical and infrastructural conditions.

3.1. Model initialization

The pipeline begins in northern Italy, at an oil storage facility near Trieste and ends in southwestern Germany at the MiRO refinery in Karlsruhe. The exact coordinates are provided in **Appendix B.4**. The set diameter, resulting mass flows, and pump intervals are shown in Table 1.

The WACCs for the traversed countries range between 5 and 7% (6.9% Italy, 5.9% Slovenia, 5.1% Austria, and 4.7% Germany) [36,42]. The corresponding pump interval calculations are documented in the **Supplementary data S1**.

3.2. Routing

The linear distance between the start (Trieste) and end point (Karlsruhe) is 568 km. The modelled pipeline is generally 18-22% longer than the linear distance. Hydrogen exhibits the longest route (686 km), and CO_2, FT crude, methanol, and kerosene are shorter (679 km) for a newly constructed pipeline, while CO_2 follows the shortest path (672 km) for a repurposed pipeline (Fig. 3).

For all fluids and both pipeline configurations, the pipeline route simultaneously minimizes exposure to high elevation (Fig. 4), steep slopes (**Figure B.4)**, high population density (**Figure B.5**), and intensive land use (**Figure B.6**). At the same time, it shortens the total transport distance and uses existing oil and gas pipeline corridors where economically feasible, helping to reduce the overall LCOT.

For the new pipeline, the routing is almost the same for FT crude, methanol, and kerosene. In contrast, hydrogen follows a different path over the final 100 km, bypassing densely populated and intensively used areas while maximizing use of existing infrastructure instead of taking the direct route. Immediately after entering Germany, CO_2 traverses areas with slightly higher elevation (between 300 and 500 height metres, see Fig. 5a) and exhibits even greater alignment with existing infrastructure (see Fig. 4a). For all fluids, the new pipeline aligns with existing infrastructure for up to two-thirds of its length, making use of Right-of-Way (ROW). However, it deviates from the existing TAL pipeline for almost half of the route (Fig. 4a). This deviation arises in part because the TAL system supplies refineries in Bavaria and Austria, which are not considered as boundary conditions in this case study. As hydrogen and CO_2 are transported at higher pressures than the liquid hydrocarbons, their pipelines have higher CAPEX and are therefore more reliant on existing infrastructure to minimize costs.

For the repurposed pipeline, all fluids follow a very similar route. In this configuration, the pipeline fully aligns with existing infrastructure apart from the start tile. Notably, the repurposed pipeline diverges from the TAL about one-third of the route and takes a shortcut after the German-Austrian border to connect with a gas pipeline system before rejoining the TAL corridor near Karlsruhe (Fig. 4b). The route of the gas [43] and oil [44] pipeline is taken from the © Global Energy Monitor.

The start tile lies in mountainous terrain at a mean elevation of 412 m. For the new pipeline, all fluids follow a similar elevation profile, while in the repurposed configuration methanol, FT crude, and kerosene follow the TAL corridor (Fig. 5a). Hydrogen takes a more direct coastal route within the TAL corridor, and CO_2 routes via Slovenia due to lower infrastructure use and WACC (Fig. 5b).

Route adjustments to minimize elevation change are visible in the average elevation per tile (**Figure B.2**) and the elevation profiles (Fig. 5). Except for kerosene, the new pipeline has slightly more elevation gains (Fig. 5a) than the repurposed option, where existing oil and gas infrastructure dominates route selection (Fig. 5b).

3.3. Pressure losses

FT crude requires the highest pump power (84 MW new, 92 MW repurposed), while hydrogen requires the least (10 MW new, 14 MW repurposed). Repurposed pipelines typically exhibit slightly higher

Table 1
Case study – Model initialization: Settings.

	Symbol	Unit	H_2	CO_2	MeOH	FT crude	Kero
Diameter	D_f	Inch (mm)	20 (508)				
Throughput	$\dot{m}_f$	kg/s (Mt/yr)	11 (0.3)	572 (16.9)	515 (14.8)	502 (14.4)	525 (15.1)
		TWh/yr	10	-	81	171	180
Pump interval	l_f	km	500	100	60	45	60

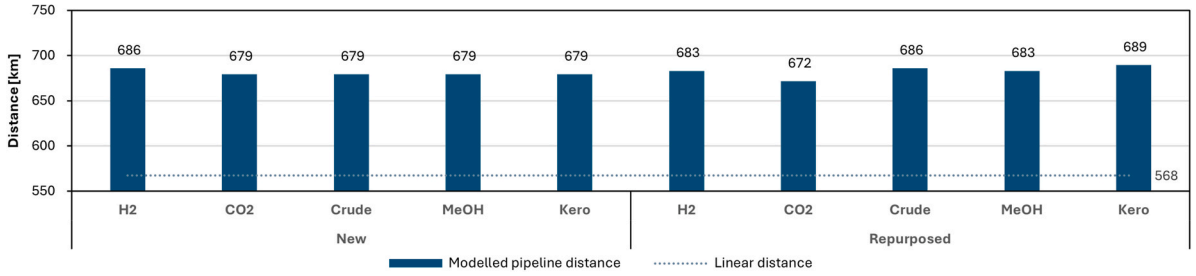


Fig. 3. Case study – Modelled pipeline distance compared to linear distance between Trieste and Karlsruhe.

pressure losses due to increased wall roughness and longer routes, except for CO_2 pipelines where elevation effects are more pronounced (Fig. 6). These values reflect the fluid-specific viscosities, indicating that higher viscosity leads to greater frictional losses, as observed for FT crude. Frictional losses are further amplified when using repurposed pipelines.

By converting pump power into pump capacity based on 8000 FLH (see **Table B.3**) and normalizing it by the energetic throughput (see Table 1), it becomes evident that approximately 0.8% (1.1%) of the hydrogen's energy equivalent is consumed for compression in new (repurposed) pipelines. In comparison, the corresponding shares are 0.6% (0.9%) for methanol, 0.4% (0.4%) for FT crude, and 0.3% (0.4%) for kerosene. These results indicate that hydrogen exhibits the highest transport-related energy losses among the fluids considered. It should be noted that transport losses due to leakage are not accounted for in this analysis.

3.4. Levelized cost of transport (LCOT)

The analysis of the LCOT in a 20-inch pipeline between Trieste and Karlsruhe reveals a pronounced economic advantage for pipeline transport of liquids and in repurposing existing pipelines compared to constructing new ones.

For hydrogen, repurposing pipelines reduces the mass-specific LCOT from 0.38 to 0.13 €$_{2023}$/kg (Fig. 7a) and the energy-specific LCOT from 11.4 to 3.9 €$_{2023}$/MWh$_{lhv}$ (Fig. 7b), corresponding to an approximate cost reduction of 65%.

Similar results are observed for the liquids FT crude, methanol, and kerosene. The new pipeline exhibits a mass-specific LCOT value of around 0.01 €$_{2023}$/kg (Fig. 7a), whereas the repurposed pipeline has lower figures of around 0.005-0.006 €$_{2023}$/kg (Fig. 7b), effectively reducing costs between one third and up to 50%. Energy-specific LCOT for liquid hydrocarbons range from 0.8 to 1.9 €$_{2023}$/MWh$_{lhv}$ for new pipelines and from 0.4 to 1.0 €$_{2023}$/MWh$_{lhv}$ for repurposed ones (Fig. 7b). CO_2 has the highest LCOT among carbon containing fluids and further increases LCOT when existing infrastructure must be followed.

These differences reflect the favourable physical properties of liquids and especially kerosene, such as moderate viscosity, high density, and relatively low operating pressure. This results in moderate CAPEX and low transport costs. Repurposing further enhances their economic advantage. FT crude is well-suited for energetic imports, especially with existing pipelines. For chemical feedstock imports, methanol is preferred, while FT crude has an advantage in repurposed infrastructure. Transporting CO_2 results in the highest LCOT due to the high pressure required, low reuse potential of existing infrastructure and thus high CAPEX. Pipeline CAPEX are the dominant cost component for hydrogen transport (Fig. 7c). In contrast, both pipeline and pump CAPEX are the primary cost drivers for transporting liquids. Together, pipeline and pump/compressor depreciation account for roughly 60% of the total LCOT in new and repurposed hydrogen and CO_2 pipelines, and newly constructed liquid pipelines. However, there is a shift in the cost structure for repurposed FT crude, methanol, and kerosene pipelines: pump-related CAPEX and variable OPEX become the main contributors, representing approximately 75% of the total LCOT.

Further results on pressure losses and LCOT are provided in the **Supplementary data S2**.

3.5. Sensitivity analysis

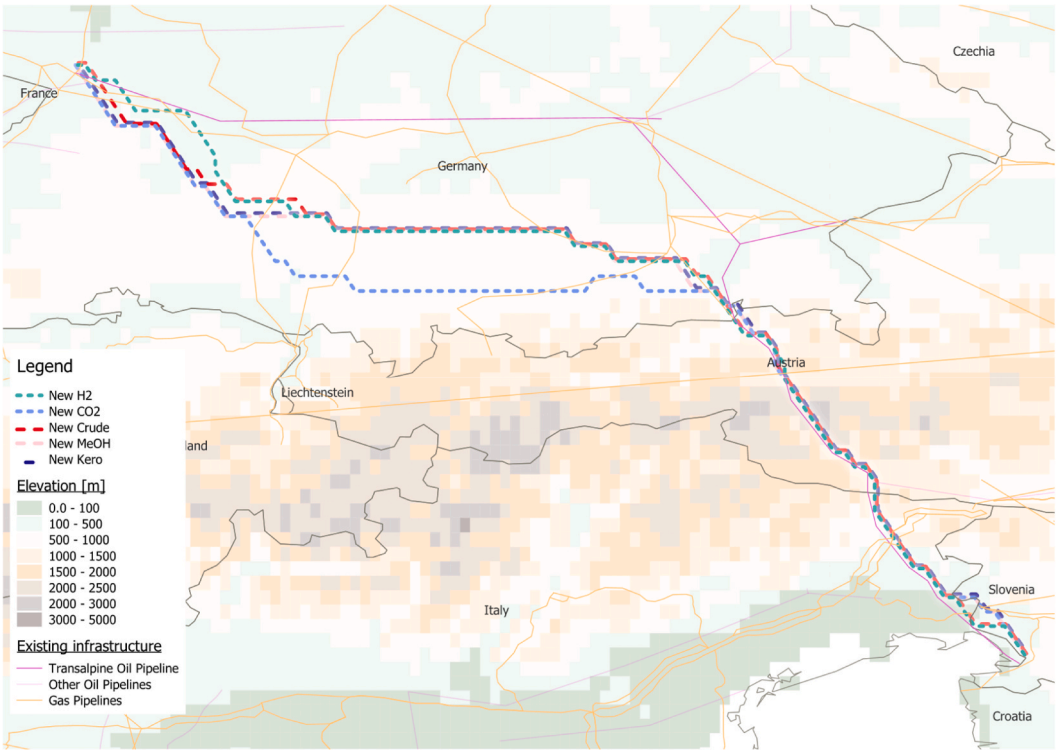
To identify the key parameters influencing LCOT, a sensitivity analysis was conducted by varying pipeline and pump CAPEX, WACC, elevation-related pump factor, and electricity prices for new pipelines, and cost factors for repurposed pipelines by ±50%. Additionally, a no-elevation case was included to assess the elevation effects. Parameter values are listed in **Table B.5**.

The results show that the LCOT for hydrogen, CO_2, and hydrocarbons is mainly driven by pipeline CAPEX, WACC, and infrastructure reuse. Pipeline CAPEX have the strongest impact, changing LCOT by up to ±47% for hydrogen and ±35% for liquids. Pump CAPEX affect LCOT by up to ±9% for liquids, especially high-pressure fluids, and ±3% for hydrogen. Changes in WACC have a significant influence on LCOT (up to ±20%). Electricity prices have limited influence on hydrogen (±3%) and moderate impact on liquids (±7 to ±10%). Decreasing the pipeline repurposing cost factor reduces the LCOT by up to 34% for hydrogen and CO_2, and 17% for hydrocarbons. Assuming flat terrain for constructing a new pipeline decreases the LCOT for liquids by 3 to 5% but has no effect on hydrogen. The results are shown in Fig. 8.

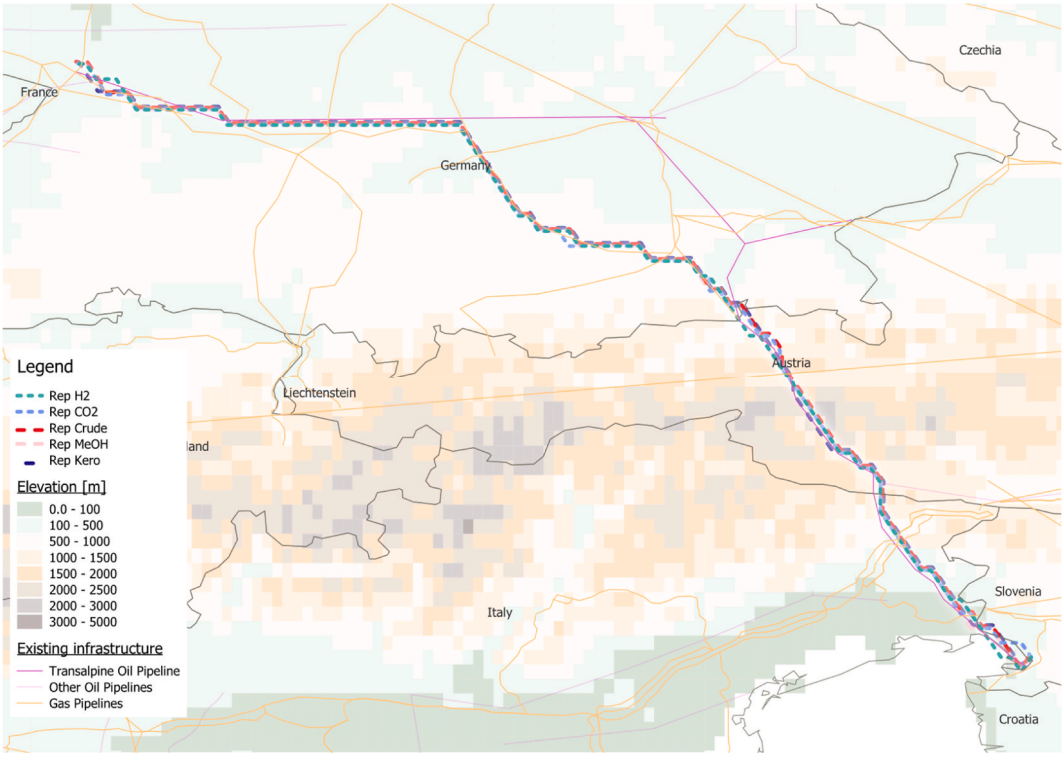
Routing outcomes remain largely stable across all sensitivity cases and exhibit only minor local deviations. Slightly more direct alignments occur in the Alpine region under no-elevation assumptions, while noticeable rerouting is observed only for CO_2 under a reduced pump elevation factor and for hydrogen under high pipeline CAPEX. For all other fluids and for variations in repurposing cost factors, routing effects are negligible.

4. Discussion

This section summarizes the key findings from the case study, uses a comparison with other studies to evaluate the robustness of the results, and discusses the limitations of this study.



(a)



(b)

Fig. 4. Case study - Routing map with the existing oil and gas pipeline infrastructure and elevation for (a) new and (b) repurposed pipeline configuration.

4.1. Key findings

The model calculates optimal routes and LCOT for different fluids and pipeline types using GIS-based data and pressure loss analysis. A case study of a 20-inch pipeline from Trieste to Karlsruhe demonstrates how elevation and pressure losses influence LCOT. Two pipeline strategies were evaluated: constructing new infrastructure versus repurposing existing pipelines.

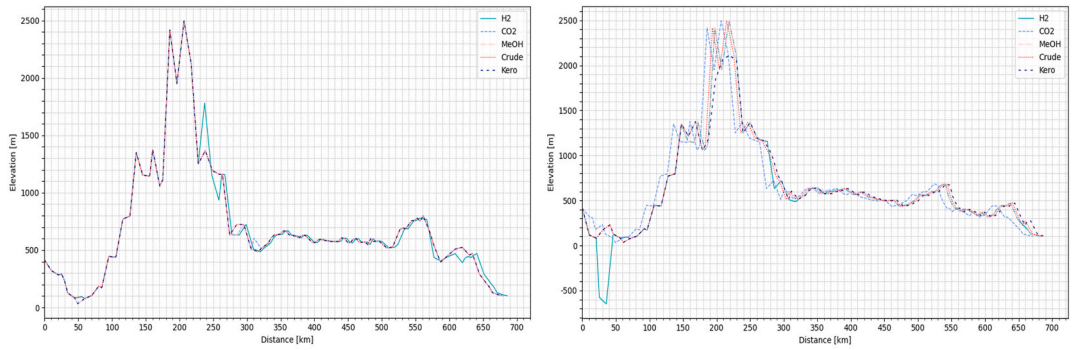


Fig. 5. Case study - Elevation profile for (a) new and (b) repurposed pipeline configuration.

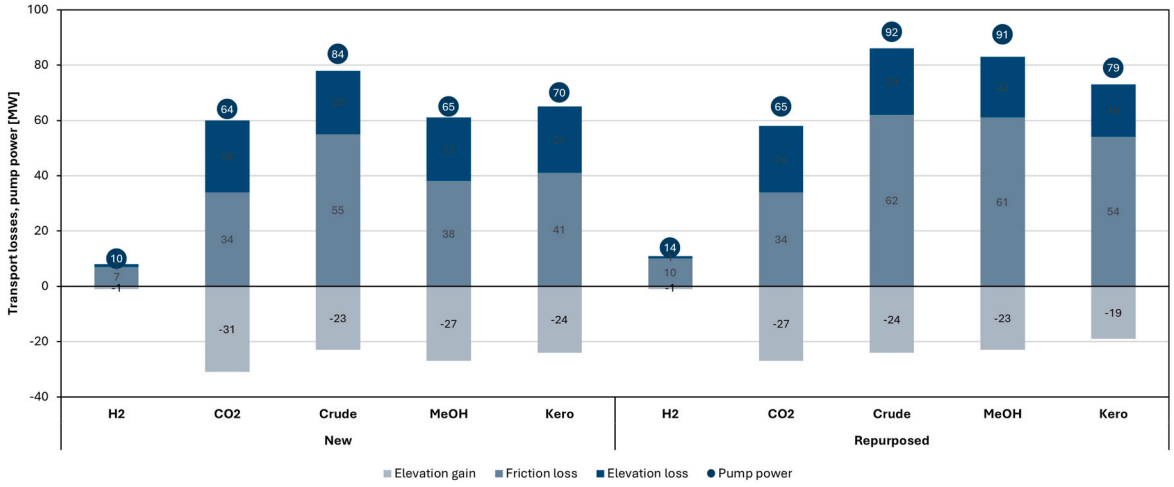


Fig. 6. Case study - Pressure losses and required pump power for new and repurposed pipeline configuration.

- **Routing:** Routes are 18-22% longer compared to the linear distance (568 km) and designed to avoid densely populated areas, sensitive land use areas, and steep terrain. In our case study, the newly constructed pipeline has up to 66% alignment with existing gas and oil infrastructure, while the repurposed pipeline has nearly full alignment.
- **Pressure losses:** Liquids require significantly more pumping power than hydrogen due to their higher density and viscosity. In relative terms, however, compression consumes about 0.8% (1.1%) of hydrogen's energy content, compared to 0.6% (0.9%) for methanol, 0.4% (0.4%) for FT crude, and 0.3% (0.4%) for kerosene in new (respectively, repurposed) pipelines.
- **LCOT:** Liquid fuels are more cost-efficient than hydrogen due to their higher energy density. Hydrogen transport is up to 35 times more expensive per kg and 10 times more expensive per MWh. Kerosene has the lowest LCOT due to its high compatibility with the existing infrastructure and low CAPEX. FT crude is also economical to transport, especially in repurposed pipelines. Methanol is more cost-effective per kilogram, while FT crude is more economical per MWh. CO_2 transport remains costly due to its high pressure requirements and CAPEX, which make repurposing impractical. The sensitivity analysis shows that flat terrain may decrease the LCOT for liquids.

4.2. Model validation

There is no existing study that jointly accounts for routing, pressure losses, and fluid-specific parameters across several carrier types. Our work fills this gap and includes pipeline repurposing for liquid hydrogen derivatives. A literature review [28] highlights three relevant works: DeSantis et al. [29], Galimova et al. [45], and Papadias et al. [20].

- DeSantis et al. [29] compare transmission costs for oil, ethanol, methanol, natural gas, and hydrogen in a 36-inch, 1,608 km pipeline at 8% WACC. Normalized to 1,000 km, oil is cheapest (0.5 $€_{2023}$/MWh_{lhv}), followed by methanol (1.2) and hydrogen (2.5), while electricity transmission is substantially higher (24.3). Their study does not account for routing or geographical constraints.
- Galimova et al. [45] analyse green methanol supply via European production, pipeline imports from Morocco, and maritime shipping. LCOT depend strongly on the assumed capacities (15–51 TWh/yr) and WACC (5–9%). CAPEX are based on fossil fuel projects and include a 20% detour factor but no modelling of pressure losses. Normalized costs range from 3.2 to 6.9 $€_{2023}$/MWh_{lhv}. The diameters in Fig. 9 are estimated based on Eq. 2.
- Papadias et al. [20] examine pipeline transport costs for gaseous hydrogen and several derivatives over 3,500 km. They assume a fixed WACC of 10%, and pipeline CAPEX are based on the Hydrogen Delivery Scenario Analysis Model (HDSAM) [46]. Their LCOT results range from 7.8 to 8.8 $€_{2023}$/MWh for hydrogen (2-6 Mt/yr) and from 2.4 to 5.4 $€_{2023}$/MWh (10-31 Mt/yr) for methanol. Pressure losses are represented in a simplified manner, but no route-specific analysis is included.

Despite varying assumptions in the literature regarding diameter,

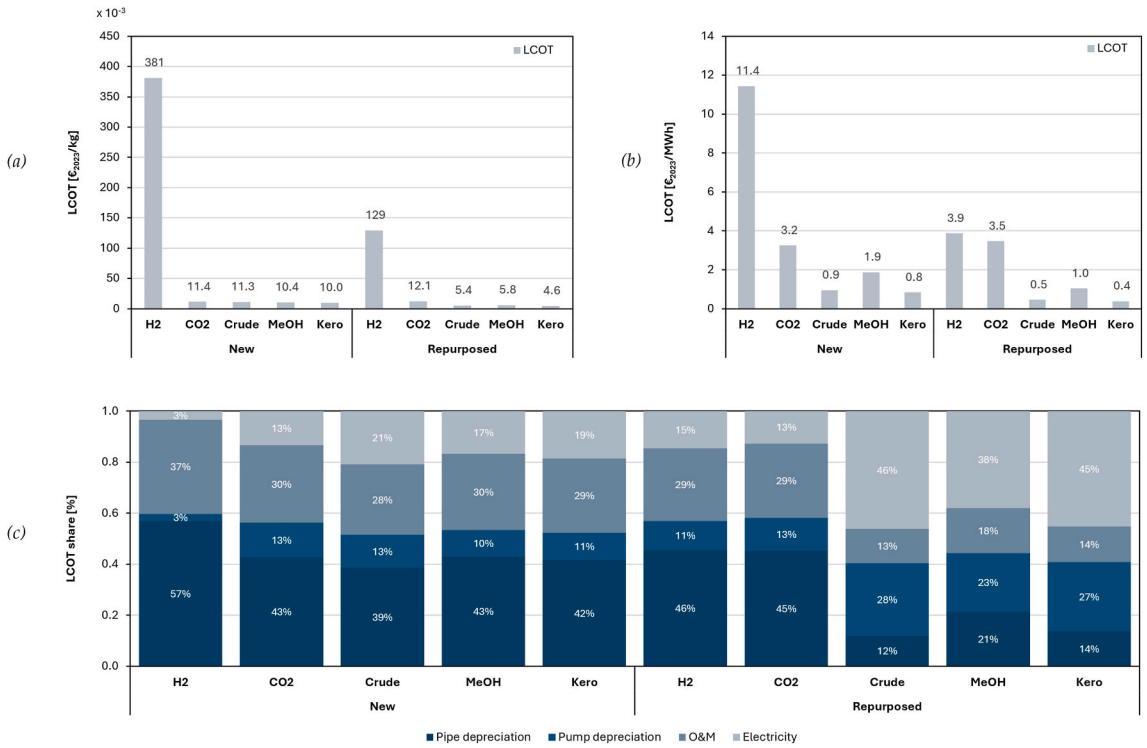


Fig. 7. *Case study – LCOT for new and repurposed pipeline configurations: (a) total LCOT in €$_{2023}$/kg, (b) total LCOT in €$_{2023}$/MWh, and (c) cost breakdown shown as relative shares in %.*

Note: Although CO_2 has no intrinsic heating value, a fictitious lower heating value of 3.5 kWh_{lhv}/kg is assigned to enable a meaningful comparison of CO_2 pipeline transport costs with those of the other fluids in €$_{2023}$/MWh_{lhv}. This value is derived from CO_2's mass share in methanol production (see **Table B.2**).

capacity, routing, and pressure levels, the relative trends remain consistent: hydrogen is more expensive to transport than methanol, oil (incl. FT crude) remains the cheapest, and all studies indicate clear economies of scale (Fig. 9).

Our LCOT values are higher mainly because we assume smaller pipeline diameters for hydrogen, methanol, and oil products compared to DeSantis et al. [29], who report the lowest LCOT due to the lowest specific pipeline CAPEX. Galimova et al.'s smaller methanol diameters explain their higher costs, while Papadias et al.'s use of HDSAM CAPEX [46] leads to moderate hydrogen but the highest methanol LCOT for comparable diameters. Under their low-WACC scenario, Galimova et al.'s [45] methanol LCOT (16 inch) aligns closely with ours (20 inch) due to similar CAPEX assumptions.

4.3. Comparing pipeline and shipping costs

To evaluate the competitiveness of pipeline-based imports, we compared our calculated pipeline transport costs with the shipping costs reported by Genge et al. [47] (see Fig. 10). In our comparison, we refer specifically to the 25th and 75th percentiles for the transport cost spans from Ref. [47] excluding conversion (e.g. liquefaction of hydrogen, synthesis of methanol and FT products) and reconversion (e.g. gasification of liquefied hydrogen, cracking). For FT diesel (FTD), shipping costs range from 0.03 to 0.3 €$_{2023}$/MWh/1,000 km. In contrast, our estimated pipeline transport costs for FT crude are substantially higher: 1.4 for new and 0.7 €$_{2023}$/MWh/1,000 km for repurposed pipelines. The shipping costs for liquefied hydrogen range from 1.2 to 13.4 €$_{2023}$/MWh/1,000 km. Our pipeline transport estimates for gaseous hydrogen fall within this range, amounting to 16.7 (new) and 5.7 €$_{2023}$/MWh/1,000 km (repurposed). Methanol shipping costs are reported to lie between 0.1 and 0.8 €$_{2023}$/MWh/1,000 km. In comparison, our pipeline transport costs are at least twice as high, with 2.8 (new) and 1.5 €$_{2023}$/MWh/1,000 km (repurposed).

Our findings show that pipeline transport, particularly for newly constructed infrastructure, is generally more expensive than shipping. Pipeline transport costs for FT crude and methanol exceed shipping costs by a factor of two or more. Although pipeline transport of gaseous hydrogen falls within the cost range of liquefied hydrogen shipping, it remains at the upper end when new infrastructure is required.

However, a direct comparison between pipeline and shipping in this case is challenging because the studies differ not only in transport distance but also lack consistent capacity assumptions, LH_2 liquefaction and regasification costs are not included, and there is no direct maritime link for the route under consideration. Our case study assumes a pipeline distance of approximately 700 km designed for a capacity of 0.3 Mt/yr hydrogen and 15 Mt/yr hydrocarbons. In contrast, the shipping routes analysed by Genge et al. [47] span 2,500 to 24,000 km. However, no annual capacity figures are provided, further complicating the comparison. As outlined in the motivation for this study, shipping becomes increasingly competitive for very large distances. For the case examined, a meaningful comparison should consider the entire supply chain, including pipeline transport versus combined shipping and inland navigation, and be based on similar distance and capacity assumptions.

4.4. Limitations of this study

This section reflects on modelling and case study limitations related to (1) technical and (2) economic simplifications, and (3) the routing approach. While these aspects may influence the local routing of new pipelines, they do not substantially affect absolute cost levels, and the relative LCOT ranking across fluids and the routing of repurposed pipelines remain robust.

(1) **Technical assumptions:** A uniform pipeline diameter of 20 inches is assumed for comparability, although existing TAL diameters range from 26 to 40 inches. With a constant throughput,

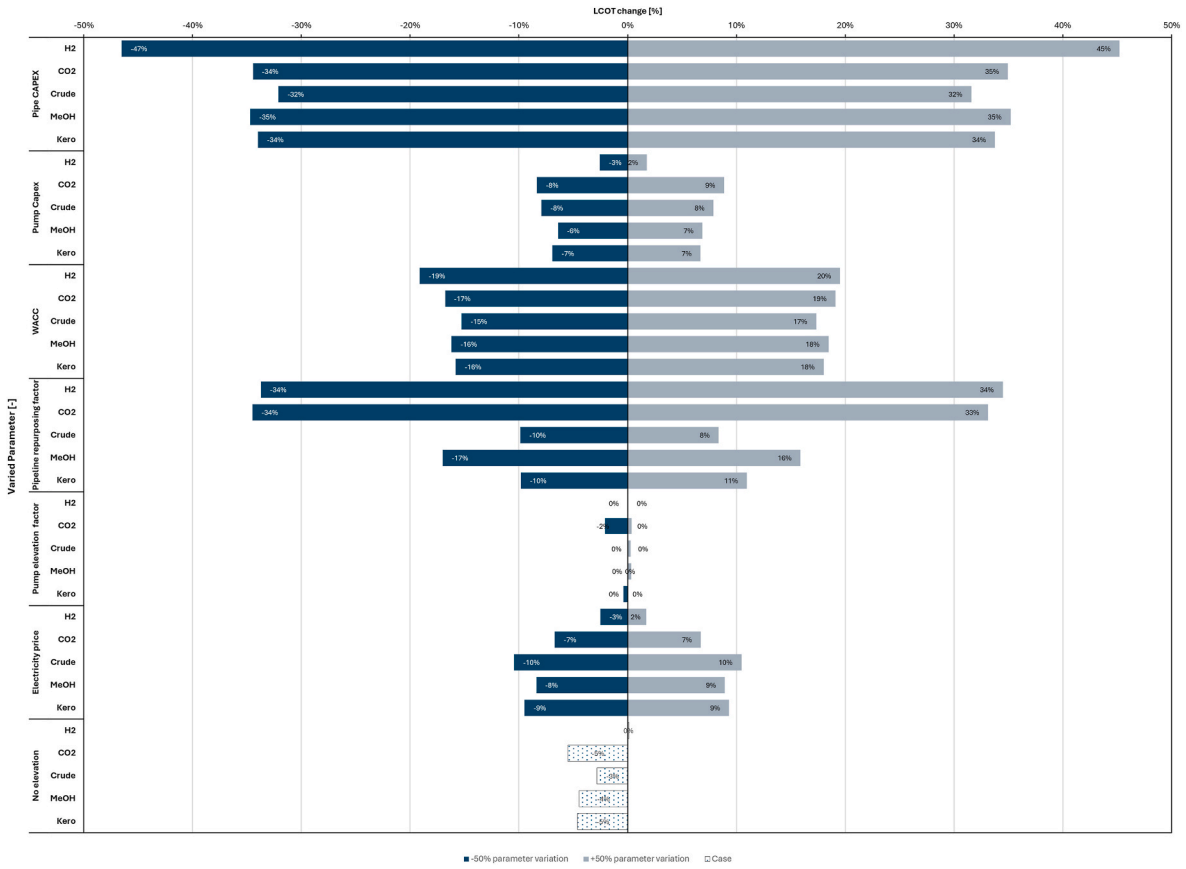


Fig. 8. Case study - Sensitivity analysis.
Note: The parameters in the sensitivity analysis were varied to compare their respective LCOT outcomes against the LCOT results of the new pipeline configuration. The only exception is the parameter "pipeline repurposing factor", which is compared against the LCOT results of the repurposed pipeline configuration.

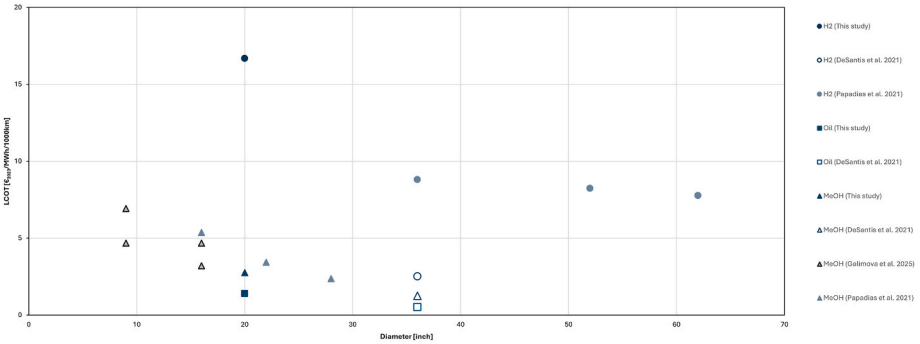


Fig. 9. LCOT comparison between this study, DeSantis et al. [29], Galimova et al. [45], and Papadias et al. [20]
Note: The converted LCOT values are taken from [27]. MeOH – methanol; oil (products) refers to FT crude in our study; DeSantis et al.: oil (products) refers to crude oil. Galimova et al.: LCOT values for methanol are shown for lower (5%) and higher (9%) WACC assumptions; Papadias et al.: The hydrogen content in methanol was calculated stoichiometrically.

using larger diameters or allowing variable flow conditions for hydrogen would increase CAPEX and LCOT. This means that our current LCOT estimates are likely on the low side, especially for hydrogen (see **Supplementary data S2**). Introducing *n-1* pump redundancy would marginally increase absolute costs but does not materially affect relative cost relationships, as pump-related costs constitute only a limited share of total LCOT.

(2) **Economic simplifications:** OPEX exclude fluid-specific operational aspects such as pigging frequency. While this may increase O&M costs for liquids, they do not alter the qualitative finding that liquid transport remains substantially cheaper than gas transport. Similarly, uncertainty in pump CAPEX has only a minor influence on LCOT, as confirmed by sensitivity analyses.

(3) **Routing approach and case-study specificity:** The model is validated against the TAL pipeline, reproducing its routing along the initial section of the corridor, with deviations occurring where TAL branches toward Austrian and Bavarian refineries that are not considered in this study. Routing simplifications, such as averaged elevation per tile (6.5 × 6.5 km), disregarding parallel pipeline strings, simplified pump elevation factors, and the exclusion of soil types or geohazards, may result in locally different routes and slightly different absolute LCOT but do not alter the relative LCOT ranking. Although the Alpine import

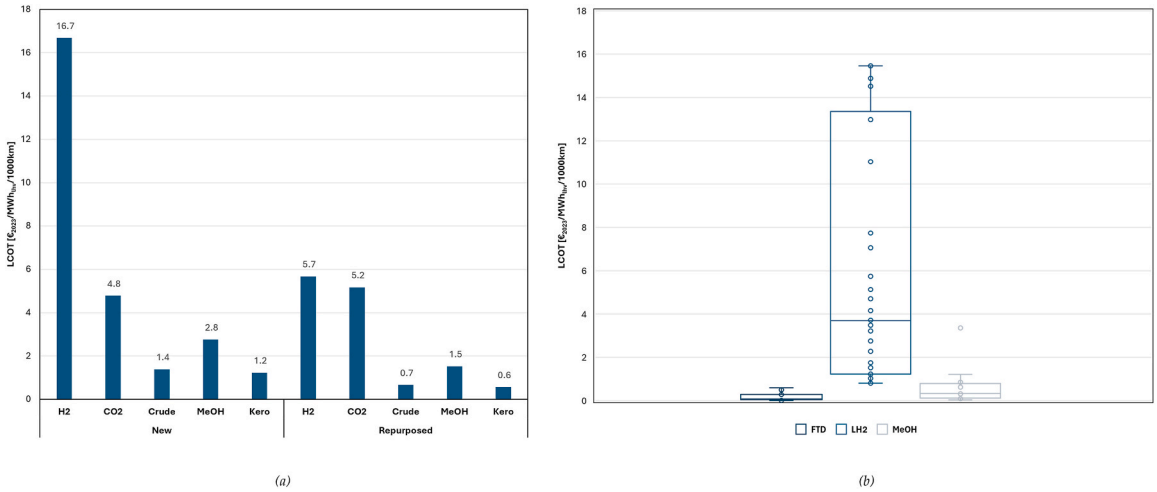


Fig. 10. LCOT comparison between (a) pipeline (this study) and (b) shipping (adapted from Genge et al. [47]).
Note: All LCOT values are normalized to 1,000 km and expressed in $€_{2023}/MWh_{lhv}$ for comparability. In this study, CO_2 was assigned a fictive lower heating value based on stoichiometric assumptions for methanol synthesis (see **Table B.2**). FTD – Fischer Tropsch Diesel, LH2 – liquefied hydrogen, MeOH - methanol. LCOT values do not include conversion or reconversion steps.

corridor analysed here is not representative of all routes, sensitivity analyses indicate that variations in terrain primarily affect routing choices rather than LCOT.

Overall, the identified limitations may influence local routing decisions or absolute cost levels minorly but do not affect the comparative LCOT results. Some assumptions would lead to alternative routes for newly constructed hydrogen or CO_2 pipelines rather than fundamentally different cost outcomes, while the dominance of pipeline CAPEX and the cost-saving potential of existing infrastructure ensure stable relative rankings across fluids and robust routing outcomes for repurposed pipelines. The model therefore provides reliable results for strategic import assessments, whereas detailed infrastructure planning remains a subject for future research.

4.5. Outlook

The case study indicates that transporting liquid hydrogen derivatives by pipeline is more cost-effective than transporting gaseous hydrogen. Future assessments should examine the number of parallel pipeline strings and evaluate additional import routes that combine shipping and pipeline transport to provide more route-specific recommendations for hydrogen and derivatives infrastructure planning.

Lower import costs for hydrogen derivatives could lead to a relocation of industrial value chains to regions where derivatives are produced. In light of transport costs, the hydrogen import volumes outlined in Germany's hydrogen strategy may need to be reassessed, particularly after further analysis of importing hydrogen (derivatives) via existing pipelines, especially for import corridors without a maritime link, and when considering the entire supply chain. In this context, existing pipelines from countries bordering the EU could be utilized. Moreover, ships and pipelines can complement each other: For instance, ships could be used for global transport to European ports, from where pipelines could then be employed for further transmission within Europe. As a result, lower hydrogen import quantities and reduced hydrogen grid capacities could be more realistic than previously assumed. However, as feedstock costs were not considered in this study, further analysis of complete supply chains is required to draw robust conclusions. This is particularly relevant for sectors that could begin value creation either from hydrogen or from its derivatives.

Further analyses of optimal transport options should also address the issue of resilience. Recent developments in the energy sector have demonstrated that the reliability of energy transport and the protection of infrastructure against various forms of disruption or attack are critical factors in comprehensive assessments.

5. Conclusions and recommendations for action

International trade in hydrogen and its derivatives will play a key role in future energy systems and this study indicates that transporting hydrogen derivatives via pipelines may offer cost and infrastructure advantages at scale, particularly in regions lacking maritime links. However, existing research has largely focused on gaseous hydrogen pipelines and the shipping of hydrogen derivatives. While direct hydrogen transport is typically more cost-effective where molecular hydrogen is required at the point of use, hydrogen derivatives can be directly utilized in sectors such as refining, chemicals, and transport. Consequently, the choice between importing hydrogen or derivatives is highly sector-specific and involves both techno-economic and strategic considerations, including regional value creation.

Current energy system studies often neglect or simplify pipeline imports of hydrogen derivatives, limiting the robustness of import strategies. This study addresses this gap by developing an enhanced modelling framework that integrates geographic, infrastructural, and techno-economic parameters for gaseous and liquid fluids and is designed to serve as an interface and input for energy system models.

Fluid-specific properties strongly influence pipeline pressure requirements, CAPEX, and the feasibility of repurposing existing infrastructure. By integrating spatial data with Dijkstra-based routing, the model enables comparative LCOT assessments for hydrogen, CO_2, FT crude, methanol, and kerosene, while remaining readily adaptable to additional fluids. The case study of a 20-inch pipeline between Trieste and Karlsruhe demonstrates that liquid fuels can achieve significantly lower LCOT despite higher pumping requirements. Transporting gaseous hydrogen can be up to 35 (10) times more expensive per kilogram (MWh) than transporting liquid hydrogen derivatives, reflecting hydrogen's low energy density. Repurposing oil and gas infrastructure generally offers major cost advantages, although it is unsuitable for CO_2 transmission due to higher pressure requirements. In new pipelines, the average transport cost of gaseous hydrogen is 556 $€_{2023}$/kg/1,000 km, compared with up to 17 $€_{2023}$/kg/1,000 km for liquid derivatives. In repurposed pipelines, the corresponding costs are 189 $€_{2023}$/kg/1,000 km and approximately 8 $€_{2023}$/kg/1,000 km. Sensitivity analyses identify pipeline CAPEX, infrastructure reuse, and WACC as the most

influential cost drivers, while electricity prices and pump CAPEX play a secondary role.

Existing literature and analyses on the pipeline transport of hydrogen derivatives are scarce and often rely on widely varying assumptions regarding diameter, distance, and capacity. This study and its results therefore contribute to the scientific discussion on transporting hydrogen and its derivatives, providing comparable properties and transparent assumptions. In particular, modelling the transport of FT crude and the reuse of existing infrastructure for derivatives remains underexplored. Overall, the identified limitations may slightly affect local routing or absolute cost levels but do not change the comparative LCOT results. Pipeline CAPEX and the cost advantages of reusing existing infrastructure ensure robust relative cost rankings across fluids. The model therefore provides reliable results for strategic import assessments, while detailed infrastructure planning remains subject to future research.

Future research should therefore incorporate GIS-based routing, infrastructure repurposing potential, throughput variability, and hybrid transport chains combining pipelines and shipping.

From a policy and infrastructure planning perspective, future analyses should adopt a system-wide approach that considers full supply chains, feedstock availability, infrastructure reuse, and resilience aspects. Importing hydrogen derivatives may reduce the need for large-scale hydrogen infrastructure in certain sectors. Overall, this study provides a foundation for improved modelling of pipeline transport and highlights the importance of fluid selection, infrastructure reuse, and route optimization for cost-effective import strategies for climate-neutral fluids.

Author contributions statement

Natalia Pieton: Conceptualisation, Methodology, Software, Data curation, Investigation, Formal analysis, Writing – original draft, Writing – review & editing, Visualization. Bastian Weiβenburger: Methodology, Software, Writing – review & editing. Lukas Karkossa: Methodology, Software, Writing – review & editing. Martin Wietschel: Writing – review & editing, Supervision. Marius Neuwirth: Writing – review & editing, Supervision.

All authors have read and agreed to the published version of the manuscript.

Declaration of competing interest

The authors declare that they have no known competing financial interests or personal relationships that could have appeared to influence the work reported in this paper.

Acknowledgements

This research was carried out as part of MOHN under grant agreement No. 03SF0675B and in cooperation with Fraunhofer CINES. During the preparation of this manuscript, the authors used ChatGPT by OpenAI and Microsoft Copilot to assist with language refinement and clarity. The authors reviewed and edited the content to ensure accuracy and take full responsibility for the final version of the manuscript.

We would like to thank Balduin Katzer from the Institute for Applied Materials (IAM) at the Karlsruhe Institute of Technology and Veronika Lenivova from the Fraunhofer Research Institution for Energy Infrastructures and Geotechnologies IEG for their insightful contributions during the initial brainstorming and conceptual development of this work. We also extend our sincere thanks to Dr. Christoph Nolden from the Fraunhofer Research Institution for Energy Infrastructures and Geotechnologies IEG for his ongoing support and guidance in his role as team leader. Furthermore, we would like to thank Gillian Brown from the Fraunhofer Institute for Systems and Innovation Research ISI for her valuable linguistic revision of the manuscript.

Appendix A. Supplementary data

Supplementary data to this article can be found online at https://doi.org/10.1016/j.esr.2026.102146.

Appendix B. Model formulation and supplementary results

B.1 Nomenclature

Abbreviation	
CAPEX	Capital expenses
CO_2	Carbon dioxide
const.	constant
DAC	Direct air capture
FLH	Full-load hours
FT	Fischer Tropsch
GIS	Geographic information system
H_2	Hydrogen
HVC	High value chemicals
Kero	Kerosene
km	Kilometre
LCOT	Levelized cost of transport
LCPA	Least cost path analysis
lhv	Lower heating value
MeOH	Methanol
MWh	Megawatt hour
O&M	Operational and maintenance costs
TAL	Transalpine Ölleitung (engl.: Transalpine Pipeline)
TWh	Terawatt hour
OPEX	Operational expenses
RE	Renewable energy
ROW	Right of Way
rep	repurposed
WACC	Weighted average cost of capital

(*continued on next page*)

(*continued*)

WC	Working capital

Symbol	Unit	
$AF^{s}_{j,i}$	-	Annuity factor for equipment j in tile i
$AF^{s}_{pipe,i}$	-	Annuity factor for pipeline in tile i and pipeline configuration s
$AF_{pump,i}$	-	Annuity factor for pump/compressor in tile i
$c_{p,f}$	$J{\cdot}kg^{-1}{\cdot}K^{-1}$	Specific heat capacity for fluid f
$CAPEX_{Pump,f}\left(P^{s}_{i,f}\right)$	$€_{2023}{\cdot}MW^{-1}$	Capacity-specific pump CAPEX for fluid f and pipeline configuration s
$CAPEX_{Pipe,f}\left(D_f, L\right)$	$€_{2023}{\cdot}km^{-1}\ m^{-1}$	Diameter-specific pipe CAPEX per km for fluid f
$CAPEX^{s}_{Pipe,i,f}$	$€_{2023}$	Pipeline CAPEX for fluid f in tile i and pipeline configuration s
$CAPEX^{s}_{Pump,i,f}$	$€_{2023}$	Pump or compressor CAPEX for fluid f in tile i and pipeline configuration s
D_f	m	Pipeline diameter for fluid f
e	-	End tile
$F^{s}_{Pipe,i,f}$	-	Pipeline cost factor for fluid f in tile i and pipeline configuration s
$F_{Pump,inst}$	-	Pump/compressor installation factor
$F_{Pump,i,elev}$	-	Elevation-specific cost factor for pumps in tile i
FLH	h	Full-load hours
g	$m{\cdot}s^{-2}$	Gravity
h_i	m	Elevation start in tile i
h_{i+1}	m	Elevation end in tile i/elevation start in tile i+1
k	mm	Pipeline roughness for pipeline configuration s
k^{new}	mm	Roughness for new pipelines
k^{rep}	mm	Roughness for repurposed pipelines
$K_{K,i}$	-	Pipeline corridor cost factor in tile i
$K_{L,i}$	-	Land use cost factor in tile i
$K_{M,i}$	-	Sea depth cost factor in tile i
$K_{P,i}$	-	Population density cost factor in tile i
$K_{S,i}$	-	Slope cost factor in tile i
$K_{m,i}$	-	Cost factor for geographic layer m in tile i
κ_f	-	Specific heat ratio for fluid f
l_f	km	Pump/compressor interval for fluid f
$L_{f,iterated}$	km	First iteration for total pipeline length for fluid f
L_i	km	Pipeline length in tile i
LHV_f	$kWh{\cdot}kg^{-1}$	Lower heating value for fluid f
$LCOT^{s}_{f}$	$€_{2023}{\cdot}kg^{-1}$, $€_{2023}{\cdot}MWh^{-1}$	Total levelized cost of transport for fluid f and pipeline configuration s
$LCOT^{s}_{i,f}$	$€_{2023}{\cdot}kg^{-1}$, $€_{2023}{\cdot}MWh^{-1}$	Levelized cost of transport for fluid f in tile i and pipeline configuration s
λ^{s}_{f}	-	Friction factor of fluid f and pipeline configuration s
M_f	$g{\cdot}mol^{-1}$	Molar density of fluid f
$\dot{m}_f$	$kg{\cdot}s^{-1}$	Mass flow of fluid f
μ_f	mPa·s	Dynamic viscosity of fluid f
$N^{s}_{i,f}$	-	Number of compression stages for fluid f in tile i and pipeline configuration s
$\dot{n}_f$	$mol{\cdot}s^{-1}$	Molar flow of fluid f
n^{s}_{j}	a	Lifetime of equipment j for pipeline configuration s
$\eta_{Comp,f}$	%	Compressor efficiency for fluid f (=hydrogen)
$\eta_{Pump,f}$	%	Pump efficiency for fluid f (=CO_2, MeOH, FT crude, Kero)
$OPEX^{fix,depr,s}_{pipe,i,f}$	$€_{2023}{\cdot}kg^{-1}$	Annual pipeline depreciation for fluid f in tile i and pipeline configuration s
$OPEX^{fix,depr,s}_{pump,i,f}$	$€_{2023}{\cdot}kg^{-1}$	Annual pump/compressor depreciation for fluid f in tile i and pipeline configuration s
$OPEX^{fix,OM,s}_{i,f}$	$€_{2023}{\cdot}kg^{-1}$	Annual operation and maintenance cost for pipeline and pumps/compressors fluid f in tile i and pipeline configuration s
$OPEX^{var}_{pipe,i,f}$	$€_{2023}{\cdot}kg^{-1}$	Annual heating pipeline OPEX for fluid f in tile i
$OPEX^{var,s}_{pump,i,f}$	$€_{2023}{\cdot}kg^{-1}$	Annual energy pump/compressor OPEX for fluid f in tile i and pipeline configuration s
$O\&M$	% of CAPEX	Operation and maintenance cost share
p_{el}	$€_{2023}{\cdot}kWh^{-1}$	Electricity price
$p_{elev,i,f}$	bar	Elevation loss for fluid f in tile i
$p^{s}_{frict,i,f}$	bar	Friction loss for fluid f in tile i and pipeline configuration s
$p^{s}_{i,f}$	bar	Pipeline inlet pressure for fluid f in tile i and pipeline configuration s
$\Delta p^{s}_{i,f}$	bar	Total pressure loss for fluid f in tile i and pipeline configuration s
$p^{s}_{i+1,f}$	bar	Pipeline outlet pressure for fluid f in tile i+1 and pipeline configuration s
$p_{max,f}$	bar	Maximum pipeline design pressure for fluid f
$p_{min,f}$	bar	Minimum pipeline design pressure for fluid f
$p_{op,f}$	bar	Pipeline inlet pressure for fluid f

(*continued on next page*)

(*continued*)

$\overline{P}^{s}_{i,f}$	MW	Average pump/compressor capacity for fluid f in tile i and pipeline configuration s
$\left\|P^{s}_{i,f}\right\|$	MW	Absolute pump/compressor capacity for fluid f in tile i and pipeline configuration s i
$P_{Comp,i,f}$	MW	Required compressor capacity for fluid f in tile i and pipeline configuration s
$P^{s}_{i,f}$	MW	Required pump/compressor capacity for fluid f in tile i and pipeline configuration s
$P^{s}_{Pump,i,f}$	MW	Required pump capacity for fluid f in tile i and pipeline configuration s
R	$J{\cdot}mol^{-1}{\cdot}K^{-1}$	Universal gas constant
Re_f	-	Reynolds number for fluid f
ρ_f	$kg{\cdot}m^{-3}$	Density for fluid f
$T_{b,f}$	K	Base temperature for fluid f
T_f	°C	Fluid temperature for fluid f
ΔT_f	K	Temperature difference between ambient and fluid f
$TCI^{s}_{Pipe,i,f}$	$€_{2023}$	Total capital pipeline investment for fluid f in tile i and pipeline configuration s
$TCI^{s}_{Pump,i,f}$	$€_{2023}$	Total capital pump/compressor investment for fluid f in tile i and pipeline configuration s
v_f	$m{\cdot}s^{-1}$	Flow velocity for fluid f
$v_{opt,f}$	$m{\cdot}s^{-1}$	Economically optimal flow velocity for fluid f
$WACC_i$	%	Weighted average cost of capital in tile i
WC	% of CAPEX	Working capital
x_f	-	Compression ratio per stage for fluid f
Z_f	-	Gas compressibility factor for fluid f
ξ	-	Discharge coefficient for pipeline friction losses

Indices	
Subscript	
i	tile
i+1	Neighbouring tile
j	Equipment (=pump/compressor, pipeline)
f	Fluid
m	Geographic layer (=slope, sea depth, population density, land use, and pipeline corridors)
Superscript	
s	Pipeline configuration (=new, repurposed)

B.2 Data input

B.2.1 Geographical factors

The geography-specific cost factors K_m reflect various routing constraints m, including slope (S), sea depth (M), population density (P), pipeline corridor (K), and land use (L). If no such corridor is used, a penalty factor ($K_{K,i}$) may be applied to increase CAPEX by 100%. When a pipeline corridor is crossed, the land use factor is adjusted accordingly. Further details are provided in the original HyTROM model description [36].

Table B. 1
Input parameters: Geographical factors, adapted from [36].

Geographical factors								
	Symbol	Unit	**H_2**	**CO_2**	**MeOH**	**FT crude**	**Kero**	**Source, Note**
Slope	$K_{S,i}$	-	1-4					1)
Sea depth	$K_{M,i}$	-	1-99					1)
Population	$K_{P,i}$	-	1-99					1)
Land use	$K_{L,i}$	-	Outside corridor: 1-99, Within corridor: Reduced					1), 2)
Pipeline corridor	$K_{K,i}$	-	Outside corridor: 2; Within corridor: 1					1), 3)
Weighted average cost of capital	$WACC_i$	%	Country specific					1)

Notes:
1) See the original HyTROM model description by Ref. [36].
2) Land use cost factors are reduced within existing pipeline corridors. Specifically, the cost multipliers for protected areas and forests are decreased by 10%. For wetlands and water crossings, multipliers of 3 and 4 are applied, respectively, instead of the standard values of 4 and 5 [36].
3) The term *corridor* refers to designated regions where pipeline infrastructure already exists.

B.2.2 Technical pipeline parameters

Within the model the fluid parameters are assumed to remain constant along the pipeline. This simplification is necessary to limit model complexity. All technical pipeline parameters are summarized in **Table B.2**.

Table B. 2
Input parameters: Technical pipeline parameters, adapted from [28].

Technical Parameters									
		Symbol	Unit	H_2	CO_2	MeOH	FT crude	Kero	Source, Note
Phase		-	-	Super-critical	liquid	liquid	liquid	liquid	1)
Temperature		T_f	°C	15	15	15	15	15	2)
Pressure	**Max**	$p_{max,f}$	bar	80.5	195.5	69[1)]	69[1)]	69	3)
	Operating	$p_{op,f}$	bar	70	170	60	60	60	4)
	Min	$p_{min,f}$	bar	30	90	>1	>1	>1	5)
Dynamic viscosity		μ_f	mPa · s	0.0088	0.1042	0.6542	7.4285	1.2315	1), 6)
Density		ρ_f	kg/m^3	5.6	942.3	801.1	773.8	821.0	1), 6)
Lower heating value		LHV_f	kWh/kg	33.3	(3.5)	5.5	11.9	11.9	7)
Specific heat capacity		$c_{p,f}$	$kJ/(kg \cdot K)$	29.14	2.12	2.47	2.05	2.01	1), 8)
Gravity		g	m/s^2	9.81					
Economic velocity		$v_{opt,f}$	m/s	9.40	3.06	3.2	3.17	3.16	9)
Roughness	**New pipe**	k_{new}	mm	0.01					10)
	Repurposed	k_{rep}	mm	0.15					10)
Specific heat ratio		κ_f	-	1.41	-	-	-	-	1)
Compressibility factor		Z_f	-	1.05	-	-	-	-	11)
Molar density		M_f	g/Mole	2.02	44.01	32.04	-	-	1)
Efficiency		$\eta_{Pump,f}$	%	75					12)
		$\eta_{Comp,f}$	%	75					12)
Universal gas constant		R	$J/(mol \cdot K)$	8.314					
Compres. ratio per stage		x_f	-	2.1	-	-	-	-	13)

Notes:
1) Data for all fluids at the specified temperature and operating pressure are sourced from Ref. [48].
2) The fluid temperature is assumed to correspond to the ambient temperature of a buried pipeline. LTFT crude is wax-like under ambient conditions [49] and requires further upgrading to meet pipeline transport specifications comparable to conventional petroleum products.
3) Maximum pressure is defined as 15% above the operating pressure. For CO_2 transport, this value can reach up to 250 bar [50] and is set to 200 bar in our analysis based on [28]. For all other liquids, values are derived from typical oil pipeline specifications [51].
4) Hydrogen transmission pipelines are economically operatable between 70 and 100 bar [52–54]. In Germany, some planned pipelines are designed for up to 120 bar [55]. For repurposed natural gas pipelines, lower operating pressures of 40–100 bar are expected [56]. A standard operating pressure of 70 bar is therefore assumed. Liquid CO_2 generally requires higher pressures of 90–250 bar for cost-effective transport [50] and is set to 170 bar in our analysis based on [28]. For methanol, FT crude, and kerosene, an operating pressure of 60 bar is assumed, based on a maximum pressure of 64 bar in oil product pipelines [51] and our own pressure-drop estimations.
5) Minimum pressures are derived from Ref. [57]. For liquid hydrocarbons, values are set above the respective vapor pressure to ensure single-phase flow [57].
6) Thermophysical properties of treated FT crude are taken from Refs. [49,58].
7) The lower heating value (lhv) is included in the parameter set to enable the conversion of the LCOT from €$_{2023}$/kg to €$_{2023}$/MWh$_{lhv}$. Lower heating values are sourced from Ref. [59]. CO_2 has no intrinsic heating value. For comparability, a fictive value was assigned based on its 88% mass share in methanol synthesis ($1\ CO_2 + 3H_2 \rightarrow 1\ CH_3OH + 1H_2O$). Given that 1 mol of methanol contains 1,18 kWh (lhv) and 1 mol of CO_2 has a mass of 44 g, this corresponds to a notional LHV of (1,18/0,044 =) 3, 5 kWh/kg for CO_2.
8) Data for FT crude and kerosene is based on [59] at ambient conditions. Treated FT crude is assumed to exhibit thermophysical properties similar to those of Diesel fuel.
9) Economic flow velocities are calculated using a regression-based approach (Eq. 1) adapted from Ref. [60].
10) Pipeline roughness values are estimated based on data from Refs. [31,60,61].
11) The compressibility factor for H_2 is taken from Ref. [62], with typical values ranging from 1.03 to 1.07 for pressures between 50 and 100 bar and temperatures from −150 °C to 100 °C.
12) Pump efficiencies are estimated from Refs. [60,63,64], H2 compressor efficiencies from Ref. [52]; Efficiencies for pumps and compressors include electrical driver losses.
13) The compression ratio per stage for H_2 (usually between 2,1 and 4,0) is adopted from Ref. [52].

The economic flow velocity is calculated using a regression-based formula derived from Ref. [60] (Eq. 1).

$$v_f = v_{opt,f} = \frac{13,729}{\rho_f^{0,219}} = const. \quad (1)$$

The model uses the outlet pressure of pumps or compressors as the operating pressure. The minimum pipeline pressure corresponds to the pump/compressor inlet pressure, while the maximum pipeline pressure includes a safety margin and is relevant for pipeline design and regulatory approval. The maximum pressure is set to be 15% above the operating pressure. In our model, we consider only intermediate booster stations and explicitly exclude any initial compressors or pumps required to raise the fluid from ambient pressure to the designated operating pressure.

B.2.3 Economic parameters

The CAPEX for pipeline and pumps/compressors are derived from pressure requirements and material specifications based on values reported in the literature [28]. Each fluid is assigned a specific maximum pipeline pressure. Pipeline CAPEX per kilometre increase with inner diameter and vary by fluid, as each fluid is operated at a defined maximum pressure level. The highest values are observed for CO_2, followed by hydrogen, methanol, and oil. Pump CAPEX, which are primarily determined by pump capacity, follow a similar trend. Here as well, higher pressure levels correspond to higher specific CAPEX. Consequently, CO_2 shows the highest specific pump CAPEX, followed by hydrogen, methanol, and oil. The regression formulas used to estimate pipeline and pump (or compressor) CAPEX are presented in **Figure B.1**.

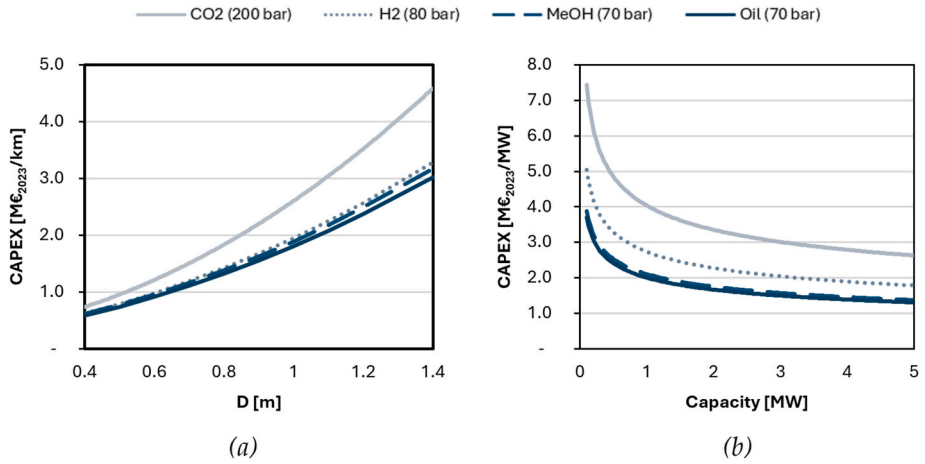


Fig. B.1. Specific CAPEX for pipelines and pumps/compressors, adapted from Ref. [28].
Notes:
a) CAPEX for pipelines were extrapolated from 80 to 100 bar natural gas systems to higher pressure levels, based on data from Refs. [65,66]. An additional 5% was added for hydrogen, CO_2, and methanol pipelines to account for material degradation due to embrittlement or corrosion [29,67]. The following regression models were derived, with x representing the inner diameter in metres and y the CAPEX in million $€_{2023}$ per kilometre - CO_2: $y = 1.8412x^2 + 0.539x + 0.2264$, $R^2 = 0.9986$; H_2: $y = 1.1112x^2 + 0.654x + 0.1839$, $R^2 = 1$; MeOH: $y = 1.0606x^2 + 0.6508x + 0.1848$, $R^2 = 1$; Oil: $y = 1.0101x^2 + 0.6198x + 0.176$, $R^2 = 1$.
b) CAPEX for pumps and compressors were extrapolated from Ref. [68] and adjusted using a pressure factor based on a reference pressure of 69 bar for natural gas systems. It is assumed that 50% of total costs are attributable to materials, and that material intensity and construction complexity are the primary cost drivers. The pressure adjustment was applied exclusively to the material cost component. The following regression models were derived, with x representing pump capacity in MW and y CAPEX in $M€_{2023}$/MW - CO_2: $y = 4.0341x^{-0,226}$, $R^2 = 1$; H_2: $y = 2.7361x^{-0,226}$, $R^2 = 1$; MeOH: $y = 2.1047x^{-0,226}$, $R^2 = 1$; Oil: $y = 2.0045x^{-0,226}$, $R^2 = 1$.

Selecting the pipeline configuration *s* (=new, repurposed) extends the original HyTROM model. For repurposed pipelines, CAPEX can be reduced to 10-90%, depending on the transported fluid. For new pipeline construction, CAPEX can be reduced to 90%, if the route follows an existing pipeline corridor. These values are based on [28] (see **Table B.3**).

Table B. 3
Input parameters: Pipeline economics, adapted from [28].

		Symbol	Unit	H_2	CO_2	MeOH	FT crude	Kero	Source, Note
Specific pipe CAPEX		$CAPEX_{Pipe,f}(D_f, L)$	$€_{2023}$/(km · m)	See fluid specific regression formula in **Figure B. 1**a)					-
Specific pump CAPEX		$CAPEX_{Pump,f}(P_{i,f})$	$€_{2023}$/MW	See fluid specific regression formula in **Figure B. 1**b)					-
Pipeline factor	**New**	$F^{new}_{Pipe,i,f}$	-	0.9					1)
	Repurposing	$F^{rep}_{Pipe,i,f}$	-	0.2	0.9	0.2	0.1	0.1	1),2)
Pump factor	***Elevation*** $\geq$ **0**	$F_{Pump,i,elev}$	-	Route: 1, LCOT: 1					3)
	Elevation $<$ **0**			Route: 0.5, LCOT: 0					
	Installation	$F_{Pump,inst}$	-	2					4)
Lifetime		n_{Pump}	yr	20					5)
		n^{new}_{Pipe}	yr	40					5)
		n^{rep}_{Pipe}	yr	30					5)
Working capital		WC	% of CAPEX	30					6)
Operation & maintenance		$OPEX^{fix,OM,s}_{i,f}$	% of CAPEX	5					7)
Full-load hours		FLH	h	8,000					8)
Electricity price		p_{el}	$€_{2023}$/kWh	0.05					Own assumption

Notes:
1) The pipeline factor only applies within a pipeline corridor – a region where pipeline infrastructure already exists – and otherwise is attributed the value 1. Constructing new pipelines along existing routes can lead to CAPEX savings of approximately 10 to 15% using RoW [28].
2) Existing pipeline infrastructure is not suitable for repurposing to transport liquid CO_2 due to the significantly higher pressure requirements, up to 250 bar [50], compared to the typical design pressure of existing pipelines, which is limited to approximately 100 bar [28]. Therefore, when considering repurposing for CO_2 transport, typically only the existing right-of-way (RoW) can be used to reduce pipeline CAPEX. In contrast, repurposing NG pipelines for hydrogen transport is considered more cost-effective (20% of new pipeline CAPEX) [28]. By analogy, repurposing CAPEX of 20% is assumed for methanol when utilizing existing pipelines. For FT crude and kerosene transport, it is assumed that only pipeline cleaning would be necessary for reuse (10% of new pipeline CAPEX) [28]. For hydrogen, see Ref. [36].
3) The pump elevation factor is the only geographical parameter that affects pump CAPEX and variable OPEX and is an own estimation. Negative elevation would theoretically result in negative pump CAPEX and OPEX; this must be corrected in the final LCOT calculation. A stepwise approach is introduced in the data processing methodology: (I) to determine the optimal pipeline route, and (II) to calculate the corresponding LCOT on the tiles along the optimal route.
4) The pump installation factor is adopted from Refs. [52,68,69].
5) Reported lifespans for pipeline infrastructure in the literature range from 15 to 55 years [50,52–54,64,65,70–73]. For pumps and compressors, the assumed operational life typically spans 15 to 25 years [50,52,70,72,74].
6) The working capital represents the additional investment required to commission the installed infrastructure. These costs are typically estimated at approximately 30% of CAPEX. An example is given in Ref. [52].
7) Reported O&M cost estimates vary by equipment type and source. Values range from 1.5% to 5% of capital costs, with pipelines typically at the lower end and compressors and pumps at the higher end [50,54,75]. A uniform rate of 5% is applied in this study to reflect the absence of explicitly accounted labour costs and to anticipate increased maintenance requirements beyond the expected service life of pumps and compressors.
8) Pipelines are generally designed for continuous operation, as confirmed by industry sources [22].

B.3 Data processing

B.3.1 Step 1: Model initialization

To initialize the model,

- the considered region is divided into tiles,
- one start and one end point are defined,
- one pipeline configuration s is chosen (new or repurposed),
- one diameter D_f (or alternatively a mass flow rate $\dot{m}_f$) is selected for all fluids, and a
- fluid-specific pump interval l_f is derived.

A dedicated spatial layer is created for each geographic parameter: population density, land use, slope, sea depth, elevation, and WACC. These layers are superimposed to form a composite grid, where each node represents a tile of 6.5 km × 6.5 km and contains all relevant geographic attributes. For further details on the geographic layering and routing optimization methodology, see Ref. [36].

To ensure comparability across different transported fluids, either the pipeline diameter D_f or the mass flow rate $\dot{m}_f$ must be fixed. If the diameter is fixed, the corresponding mass flow rates $\dot{m}_f$ are calculated using Eq. 2, which depends on the fluid-specific density ρ_f and flow velocity v_f:

$$\dot{m}_f = \frac{{D_f}^2 \cdot \rho_f \cdot \pi \cdot v_f}{4} \tag{2}$$

If the fluids are to be compared based on mass flows rather than diameter, the mass flow rate is fixed and Eq. 2 is rearranged to solve for the corresponding diameter D_f.

A preliminary pressure loss estimation is carried out on a flat pipeline profile to determine average pump intervals for each fluid (see **Supplementary data S2**). This estimation is based on the selected diameter D_f, pipe roughness k, economic flow velocity v_f, fluid density ρ_f, and viscosity μ_f, assuming no elevation changes.

B.3.2 Step 2: Pressure loss calculation per tile

The technical pipeline parameters are used to determine the pressure loss in bar per tile and fluid, denoted as $\Delta p^s_{i,f}$ (Eq. 3). The total pressure loss consists of frictional losses $p^s_{frict,i,f}$ and elevation-related losses $p_{elev,i,f}$:

$$\Delta p^s_{i,f} = p^s_i - p^s_{i+1} = p^s_{frict,i,f} + p_{elev,i,f} \tag{3}$$

Fluids may be considered incompressible if pressure loss is below 10%, or up to 40% under certain conditions [76]. Frictional losses $p^s_{frict,i,f}$ are calculated based on the length of the pipeline segment per tile L_i, the inner diameter D_f, flow velocity v_f, friction factor λ^s_f, and fluid density ρ_f (Eq. 4). The frictional losses for gases and liquids are estimated using the empirical Darcy-Weisbach formula [76]. Losses due to bends and fittings (represented by ξ) are neglected, as their influence on long-distance pipelines is considered negligible [31]:

$$p^s_{frict,i,f} = \xi \cdot \frac{v_f^2}{2} + \frac{\rho_f \cdot \lambda^s_f \cdot L_i \cdot v_f^2}{D_f \cdot 2}, with\ \xi = 0 \tag{4}$$

The fluid- and pipeline configuration-specific friction factor λ^s_f is calculated using a Colebrook–White approximation by Papaevangelou and Fang [77], which requires the Reynolds number Re_f, relative roughness k^s, and inner diameter D_f. As Eq. 5 shows, the Reynolds number increases with decreasing dynamic viscosity μ_f, and increasing density, velocity, and diameter. A higher Reynolds number generally results in a higher friction factor under turbulent flow conditions:

$$\lambda^s_f = \frac{1,613}{\left[ln\left(0,234 \cdot \left(\frac{k^s}{D_f} \right)^{1,1007} - \frac{60,525}{Re_f^{1,1105}} + \frac{56,291}{Re_f^{1,0712}} \right) \right]^2}, \text{with } Re_f = \frac{\rho_f \cdot v_f \cdot D_f}{\mu_f} \tag{5}$$

Elevation-related pressure losses $p_{elev,i,f}$ are calculated based on the elevation difference $(h_{i+1} - h_i)$ between two adjacent nodes (i+1, i), constant fluid density ρ_f, and gravitational acceleration g (Eq. 6):

$$p_{elev,i,f} = \rho_f \cdot g \cdot (h_{i+1} - h_i), with\ \rho_f = \text{const.} \tag{6}$$

Based on the total pressure loss $\Delta p^s_{i,f}$ and pump efficiency η_{Pump} the required pump capacity $P^s_{Pump,i,f}$ per tile is calculated as (Eq. 7):

$$P^s_{i,f} = P^s_{Pump,i,f} = \frac{\dot{m}_f}{\rho_f \cdot \eta_{Pump}} \cdot \Delta p^s_{i,f}, with\ \rho_f = const. \tag{7}$$

For hydrogen, compressor capacity $P^{s}_{Comp,i,f}$ is calculated using the multistage compression model from Ref. [52]. The calculation requires the outlet pressure $p_{i,f}$, inlet pressure $p_{i+1,f}$, base temperature $T_{b,f}$, universal gas constant R, specific heat ratio κ_f, compressibility factor Z_f, isentropic efficiency $n_{comp,f}$, compression ratio per stage x_f, and number of compression stages N_f (Eqs. 8-9).

$$P^{s}_{i,f} = P^{s}_{Comp,i,f} = N^{s}_{i,f} \cdot \left(\frac{\kappa_f}{\kappa_f - 1}\right) \cdot \left(\frac{Z_f}{\eta_{Comp,f}}\right) \cdot T_b \cdot \dot{n}_f \cdot R \cdot \left[\left(\frac{p_{i,f}}{p_{i+1,f}}\right)^{\left(\frac{\kappa_f - 1}{N^{s}_{i,f} \cdot \kappa_f}\right)} - 1\right], with\ p^{s}_{i,f} = p^{s}_{i+1,f} + \left(p^{s}_{frict,i,f} + p_{elev,i,f}\right) \tag{8}$$

$$N^{s}_{i,f} = \frac{\log\left(\frac{p^{s}_{i,f}}{p^{s}_{i+1,f}}\right)}{\log\left(x_f\right)} \tag{9}$$

B.3.3 Step 3: LCOT calculation per tile

One of the two pipeline configurations s is chosen: Either all pipelines along the route are newly constructed (*new*), or, if pipelines already exist along the route, they are repurposed (rep). For both configurations, pumps and compressors are assumed to be newly procured. The LCOT per tile and fluid is calculated for *repurposed* or *new* pipelines ($LCOT^{s}_{i,f}$) based on the following OPEX: depreciation of pipeline ($OPEX^{fix,depr,s}_{pipe,i,f}$) and pump infrastructure ($OPEX^{fix,depr,s}_{pump,i,f}$), fixed operation and maintenance ($OPEX^{fix,OM,s}_{i,f}$), variable costs for pumping energy ($OPEX^{var,s}_{pump,i,f}$) and optional pipeline heating ($OPEX^{var}_{pipe,i,f}$) (Eq. 10):

$$LCOT^{s}_{i,f} = OPEX^{fix,depr,s}_{pipe,i,f} + OPEX^{fix,depr,s}_{pump,i,f} + OPEX^{fix,OM,s}_{i,f} + OPEX^{var,s}_{pump,i,f} + OPEX^{var}_{pipe,i,f} \tag{10}$$

A two-step approach is introduced:

- **Step I** is used for route optimization. It includes negative pump CAPEX and OPEX to minimize edge weights.
- **Step II** is used to determine the actual LCOT for the tiles along the optimal route. It nulls negative pump CAPEX and OPEX to give realistic LCOT.

Integrating cost calculations (Step II) into the data processing as well as considering pipeline repurposing are extensions of the original HyTROM model. **Table B.4** summarizes the geographical routing factors for pipelines and pumps applied in both steps and pipeline configurations.

Table B. 4
Data processing: Pipeline and pump factors for calculating Step I and II for new and repurposed pipelines.

Pipeline configuration s	Step[1)]	Pipeline routing factors $K_{m,i}$[2)]					Pipeline cost factors $F^{s}_{Pipe,i,f}$	Pump cost factors		
								$F_{Pump,i,elev}$		$F_{Pump,inst}$
		Slope	**Sea depth**	**Population**	**Land use** [3)]	**Corridor** [4)]	[5)]	**Positive elevation**	**Negative elevation**	**Installation**
New	**I**	$K_{S,i}$	$K_{M,i}$	$K_{P,i}$	$K_{L,i}$	-	$F^{new}_{Pipe,i,f}$	1	0.5	2
	II	$K_{S,i}$	$K_{M,i}$	$K_{P,i}$	$K_{L,i}$	-	$F^{new}_{Pipe,i,f}$	1	0	2
Repurposed	**I**	$K_{S,i}$	$K_{M,i}$	$K_{P,i}$	$K_{L,i}$	$K_{K,i}$	$F^{rep}_{Pipe,i,f}$	1	0.5	2
	II	$K_{S,i}$	$K_{M,i}$	$K_{P,i}$	$K_{L,i}$	-	$F^{rep}_{Pipe,i,f}$	1	0	2

Notes.
1) Step I yields the optimal route; Step II yields the respective LCOT.
2) All values for pipeline routing factors can be found in **Table B.1**.
3) For an existing pipeline corridor, the land-use factor is reduced to the pipeline land-use factor.
4) In the repurposed configuration and Step I, a penalty factor is applied for not using an existing pipeline corridor.
5) The pipeline cost factor only applies within a pipeline corridor, a tile where pipeline infrastructure already exists. The values are presented in **Table B.3**.

Impact of negative elevation on LCOT. Geographical gradients directly affect pipeline energy demand. In the case of descending terrain, negative pump capacities may occur, potentially resulting in negative pumping-related CAPEX and OPEX. While technically plausible, such negative values pose challenges for routing algorithms such as Dijkstra, which cannot handle negative edge weights. To address this, the pump capacity is calculated by taking the absolute value to avoid negative results, and two distinct steps are implemented and applied to the *same tile*: Step I for routing and Step II for calculating LCOT. Both apply a pump cost factor $F_{Pump,i,elev}$, which adjusts CAPEX and OPEX based on elevation changes at the tile level.

In **Step I**, negative CAPEX and OPEX values, arising from downhill segments, are partially accounted for by crediting 50% of their magnitude to the

corresponding edge weight. To comply with Dijkstra's algorithm, any resulting negative total cost is set to zero, ensuring non-negative LCOT values within the routing graph.

In **Step II**, we follow a conservative accounting principle: all negative pump-related costs are set to zero in the final LCOT calculation. This prevents an overestimation of economic benefits from gravitational pressure gains and ensures that only economically justifiable cost reductions are considered.

This stepwise approach allows geographical advantages to be considered during route optimization, while preserving the integrity of the cost assessment. It ensures that routes along favourable gradients are preferred during routing without artificially lowering the LCOT. The method is especially relevant in mountainous regions where elevation has a non-negligible impact on pipeline energy performance.

Capital expenses (CAPEX) and total capital investment (TCI). Depreciation is derived from TCI, which is based on fluid-specific CAPEX. Pipeline CAPEX are now directly added to the routing algorithm, which were considered in the post-processing of the resulting route in HyTROM [36]. Pipeline CAPEX per tile ($CAPEX^{s}_{Pipe,i,f}$) for new or repurposed pipelines are calculated using a regression formula for the diameter- and length-specific pipeline CAPEX $CAPEX_{Pipe,f}(D_f, L)$ (**Figure B.1**a)), multiplied by the configuration-specific pipeline factor $F^{s}_{Pipe,i,f}$ if a pipeline exists in tile i, and adjusted by geography-specific routing factors $K_{m,i}$ (Eq. 11):

$$CAPEX^{s}_{Pipe,i,f} = F^{s}_{Pipe,i,f} \cdot CAPEX_{Pipe,f}(D_f, L) \cdot L_i \cdot \left(1 + \sum_{m} K_{m,i} - 1\right), \tag{11}$$

with $s = new, rep$; *and* $m =$ *slope, sea depth, population density, land use, pipeline corridors*

The pipeline factor is 1 if no pipeline exists in the tile. The value range of all routing factors K_m (for slope, sea depth, population density, land use, and pipeline corridors) and fluid-specific pipeline factors $F^{s}_{Pipe,i,f}$ can be found in **Table B.1** and **Table B.3**, respectively.

The pump CAPEX per tile $CAPEX^{s}_{Pump,i,f}$ are calculated by taking the absolute pump capacity to avoid negative results. Therefore, we use a fluid- and capacity-specific CAPEX regression formula $CAPEX_{Pump,f}(P_{i,f})$ (**Figure B.1**b)) based on the average pump capacity per tile $\overline{P}^{s}_{i,f}$, multiplied by the absolute pump capacity per tile $\left|P^{s}_{i,f}\right|$ and adjusted by the elevation-specific cost factor $F_{Pump,i,elev}$ (Eq. 12). $F_{Pump,i,elev}$ values are shown in **Table B.3**.

$$CAPEX^{s}_{Pump,i,f} = F_{Pump,i,elev} \cdot CAPEX_{Pump,f}\left(\overline{P}^{s}_{i,f}\right) \cdot \left|P^{s}_{i,f}\right| \tag{12}$$

The model incorporates economies of scale by averaging pump capacity over the entire pumping interval instead of calculating pump CAPEX based on the specific capacity required for each tile. For example, if a pumping interval covers 100 km and requires a total capacity of 0.1 MW, and a tile represents 10 km of that interval, the tile is assumed to contribute proportionally. The pump capacity is therefore multiplied by a factor of ten. The specific pump CAPEX in €$_{2023}$/MW are then estimated based on a 1 MW pump rather than a 0.1 MW unit. This reflects the cost advantage of larger equipment. Thus, to calculate the average pump capacity per tile, the total pump capacity per tile (Eq.s (7) and (8)) is multiplied by the fluid-specific pumping interval l_f and divided by the length of the pipeline per tile L_i (Eq. 13):

$$\overline{P}^{s}_{i,f} = \left|P^{s}_{i,f}\right| \cdot \frac{l_f}{L_i} \tag{13}$$

TCI is then calculated by applying the working capital (WC) on pipeline CAPEX (Eq. 14), as well as the pump installation factor ($F_{Pump,inst}$) and WC on pump CAPEX (Eq. 15):

$$TCI^{s}_{Pipe,i,f} = CAPEX^{s}_{Pipe,i,f} \cdot (1 + WC) \tag{14}$$

$$TCI^{s}_{Pump,i,f} = CAPEX^{s}_{Pump,i,f} \cdot F_{Pump,inst} \cdot (1 + WC) \tag{15}$$

Fixed and variable operational expenses (OPEX). Fixed OPEX include an annual depreciation for pipeline ($OPEX^{fix,depr,s}_{pipe,i,f}$) and pumps ($OPEX^{fix,depr,s}_{pump,i,f}$), and costs for operation & maintenance ($OPEX^{fix,OM,s}_{i,f}$). Annual depreciation is calculated using the annuity factor method (Eq. 16–18), which accounts for asset lifetime n^{s}_{j} and country-specific weighted average cost of capital $WACC_i$:

$$OPEX^{fix,depr,s}_{pipe,i,f} = TCI^{s}_{Pipe,i,f} \cdot AF^{s}_{pipe,i} \tag{16}$$

$$OPEX^{fix,depr,s}_{pump,i,f} = TCI^{s}_{Pump,i,f} \cdot AF_{pump,i} \tag{17}$$

$$AF^{s}_{j,i} = \frac{(1 + WACC_i)^{n^{s}_{j}} \cdot WACC_i}{(1 + WACC_i)^{n^{s}_{j}} - 1}, \text{with } j = pump, pipeline; \text{ and for pipeline } s = new, rep \tag{18}$$

The fixed annual OPEX for operation & maintenance are calculated as a percentage of total CAPEX (Eq. 19):

$$OPEX_{i,f}^{fix,OM,s} = O\&M \cdot \left(CAPEX_{Pipe,i,f}^{s} + CAPEX_{Pump,i,f}^{s} \right) \tag{19}$$

Variable OPEX include pump energy and optionally pipeline heating costs. Pumping energy costs are based on pump capacity, FLH, electricity price p_{el}, and the elevation-specific cost factor $F_{Pump,i,elev}$ (Eq. 20). Pipeline heating costs are an optional model feature and based on fluid-specific mass flow $\dot{m}_f$, FLH, heat capacity $c_{p,f}$, temperature difference ΔT_f between the fluid T_f and the environment $T_{ambient}$, electricity price p_{el}, and the ratio of tile length L_i to total pipeline length $L_{f,iterated}$, which needs to be approximated first (Eq. 21).

$$OPEX_{Pump,i,f}^{var} = P_{Pump,i,f}^{s} \cdot FLH \cdot p_{el} \cdot F_{Pump,i,elev} \tag{20}$$

$$OPEX_{pipe,i,f}^{var} = \frac{\dot{m}_f \cdot FLH \cdot c_{p,f} \cdot \Delta T_f \cdot p_{el}}{3600} \cdot \frac{L_i}{L_{f,iterated}}, with \;\; \Delta T_f = T_f - T_{ambient} \tag{21}$$

B.3.4 Step 4: Route optimization along tiles

The Dijkstra algorithm is applied to evaluate all possible routes between the defined start and end point, selecting the path with the lowest cumulative edge weights. The total LCOT per tile and fluid in Step I is assigned as the weight of each edge in the routing graph. The algorithm processes all feasible paths and identifies the optimal route that minimizes the sum of tile-specific LCOT values. The LCOT are recalculated in Step II by omitting negative CAPEX and OPEX due to downhill sections. This results in the lowest overall LCOT for each fluid along the selected route:

$$LCOT_f^s = \sum_{i=1}^{e} LCOT_{i,f}^s, with\ i = 1\ as\ start\ tile, and\ e\ as\ end\ tile \tag{22}$$

B.4 Sensitivity analysis

Table B. 5
Parameter value range for sensitivity analysis

Parameter	Symbol	Fluid	Unit	Parameter values		
				−50%	Base case	+50%
Pipe CAPEX	$CAPEX_{Pipe,H2}^{new}(20\ inch)$	H_2	k€$_{2023}$/km	402	803	1205
	$CAPEX_{Pipe,CO2}^{new}(20\ inch)$	CO_2	k€$_{2023}$/km	488	975	1463
	$CAPEX_{Pipe,Oil}^{new}(20\ inch)$	FT Crude, Kero	k€$_{2023}$/km	376	752	1128
	$CAPEX_{Pipe,MeOH}^{new}(20\ inch)$	MeOH	k€$_{2023}$/km	395	789	1184
Pump CAPEX[1)]	$CAPEX_{Pump,H2}(1MW)$	H_2	M€$_{2023}$/MW	1.368	2.736	4.104
	$CAPEX_{Pump,CO2}(1MW)$	CO_2	M€$_{2023}$/MW	2.017	4.034	6.051
	$CAPEX_{Pump,Oil}(1MW)$	FT Crude, Kero	M€$_{2023}$/MW	1.003	2.005	3.008
	$CAPEX_{Pump,MeOH}(1MW)$	MeOH	M€$_{2023}$/MW	1.053	2.105	3.1575
WACC	$WACC_i$	All	%	2.4 - 3.4%	4.7 - 6.9%	7.1 - 10.3%
Pipeline repurposing factor[3)]	$F_{Pipe,H2}^{rep}$	H_2	%	10	20	30
	$F_{Pipe,CO2}^{rep}$	CO_2	%	45	90	(135)[2)]
	$F_{Pipe,Oil}^{rep}$	FT Crude, Kero	%	5	10	15
	$F_{Pipe,MeOH}^{rep}$	MeOH	%	10	20	30
Pump elevation factor[4)]	$F_{Pump,elev}$	All	%	25	50	75
Electricity price	p_{el}	All	€$_{2023}$/kWh	0.025	0.05	0.075

Note:
1) The parameter value for pump CAPEX refers to a 1 MW pump as a representative case.
2) The pipeline cost factors for CO_2 pipelines exceed 100 percent when increased by 50 percent. Due to this unrealistic outcome, these cases are excluded from the sensitivity analysis.
3) Pipeline CAPEX reduction for repurposing along existing infrastructure.
4) Pump CAPEX reduction for downhill sections.

B.5 Routing coordinates

The pipeline begins in northern Italy at an oil storage facility in San Dorligo della Valle near Trieste (latitude: 45.6135488713083; longitude: 13.8584630613874), with the endpoint in southwestern Germany at the MiRO refinery in Karlsruhe (latitude: 49.0570441469371; longitude: 8.32222523403309). The start and endpoints are consistent with existing infrastructure data provided by Ref. [78].

B.6 Elevation frequency per tile

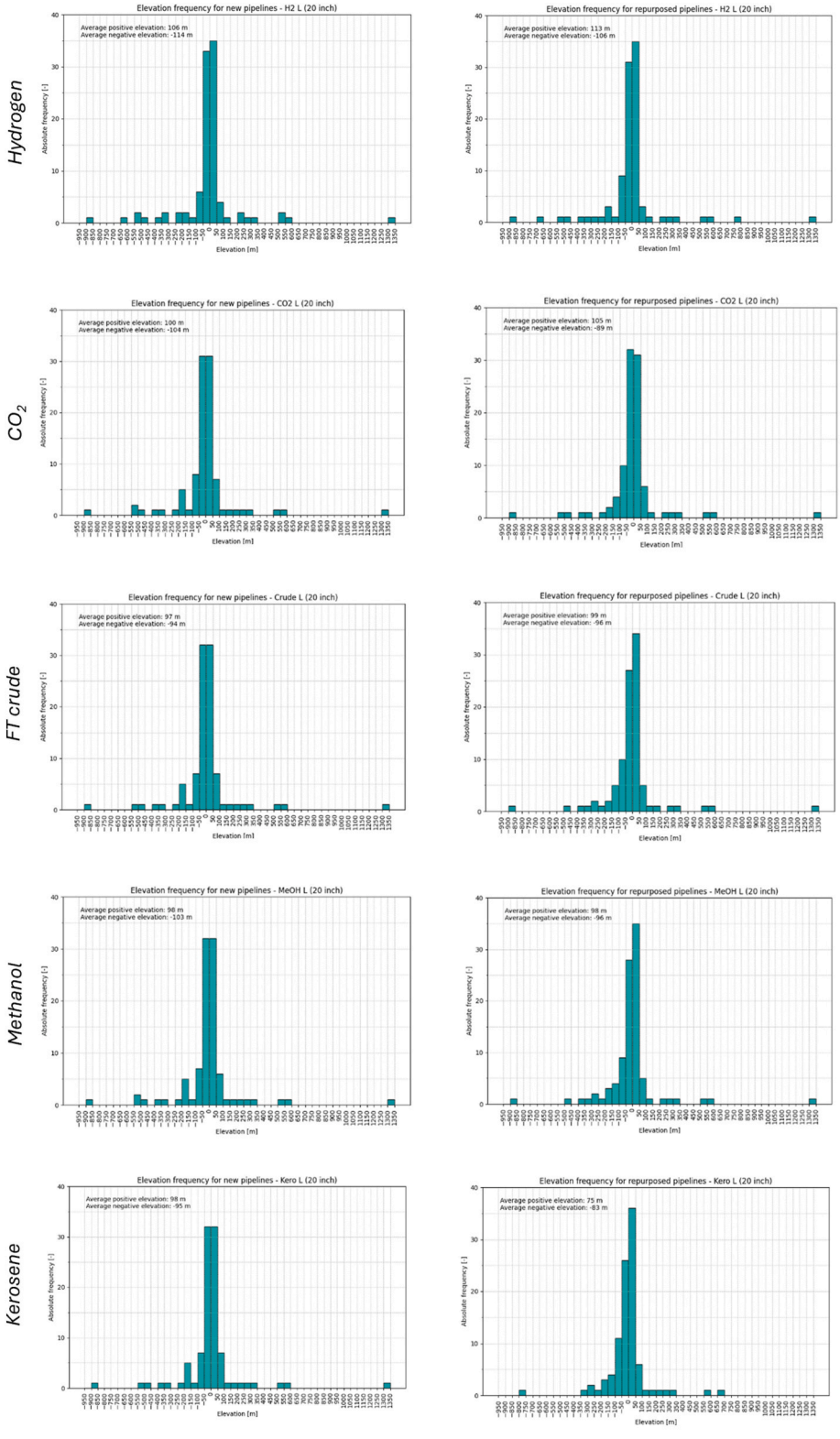
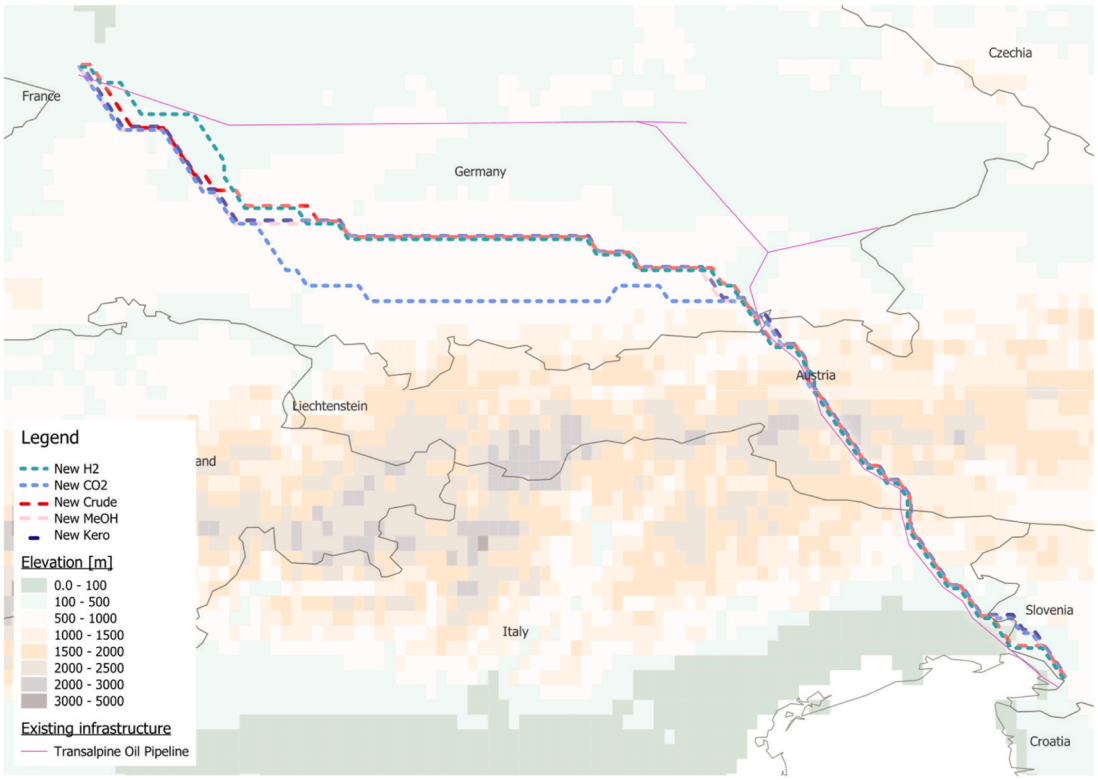
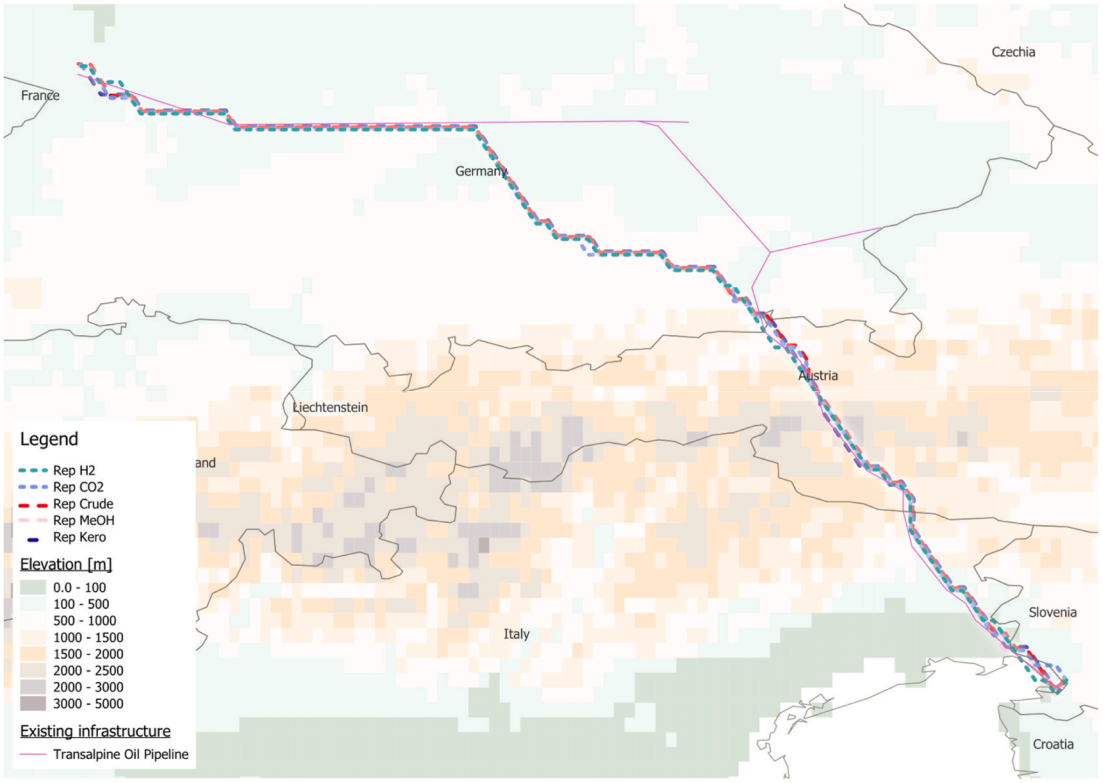


Fig. B. 2. Elevation frequency per tile for (a) new and (b) repurposed pipeline configuration.



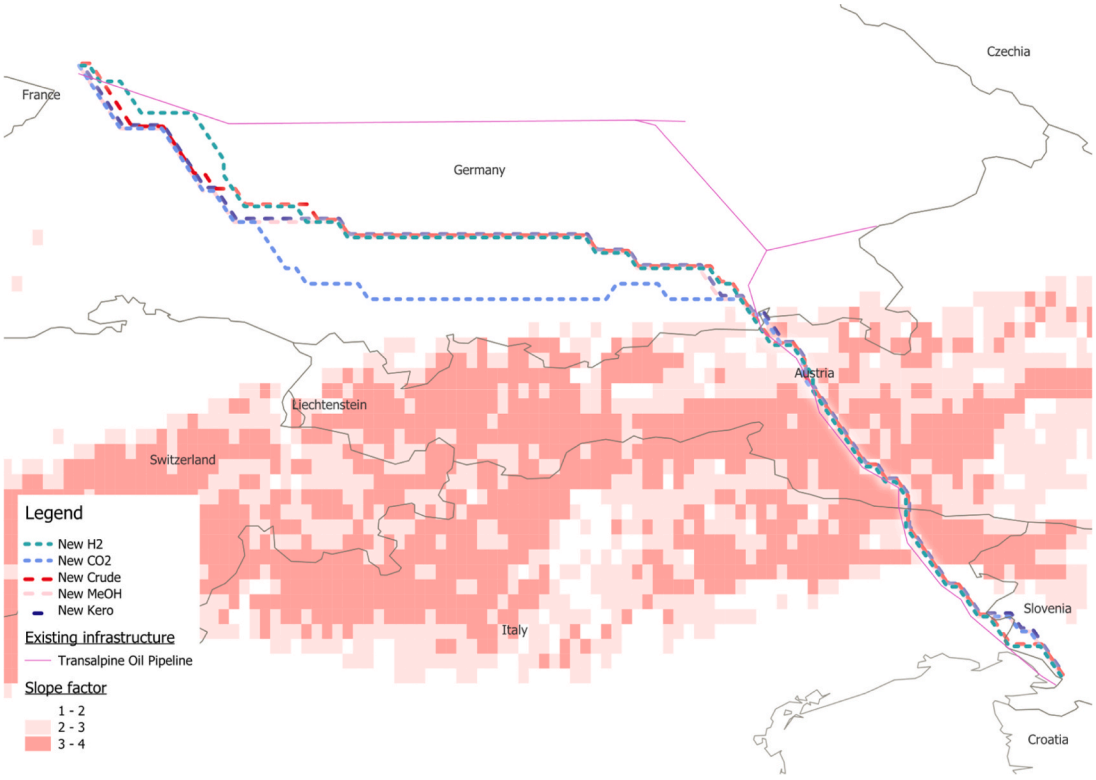
(a) New pipeline configuration



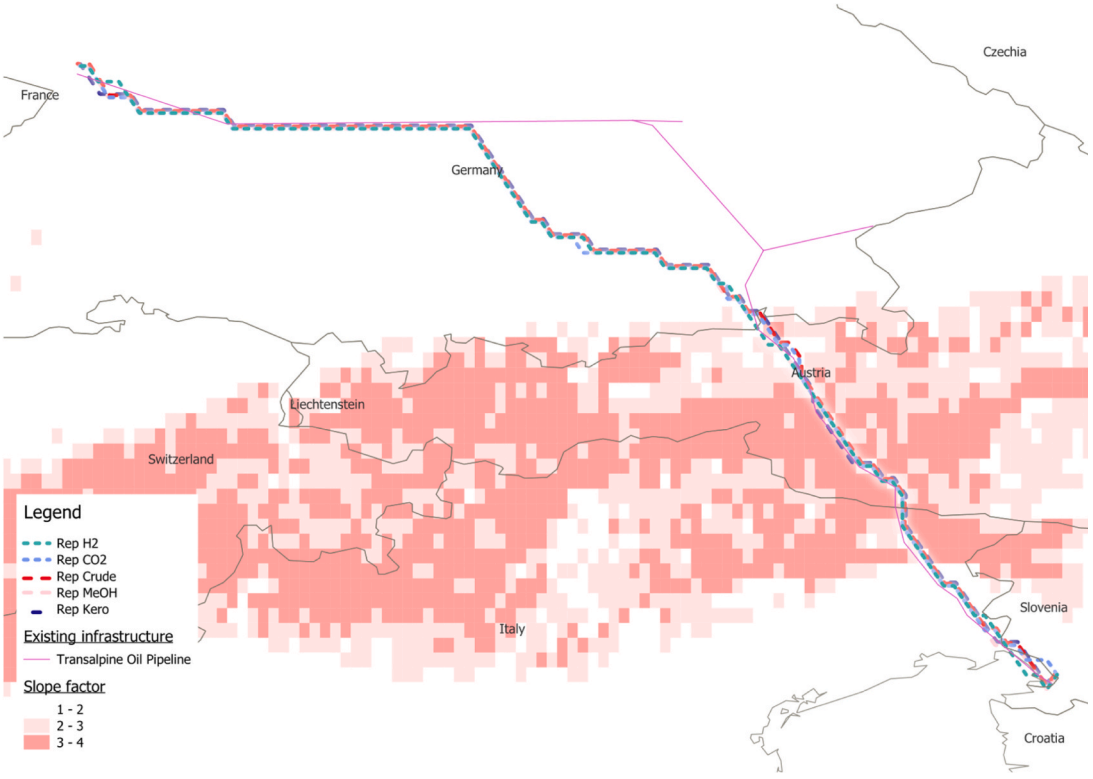
(b) Repurposed pipeline configuration (rep)

Fig. B. 3. Case study - Routing map with elevation and TAL pipeline for (a) new and (b) repurposed pipeline configuration.

B.7 Routing maps

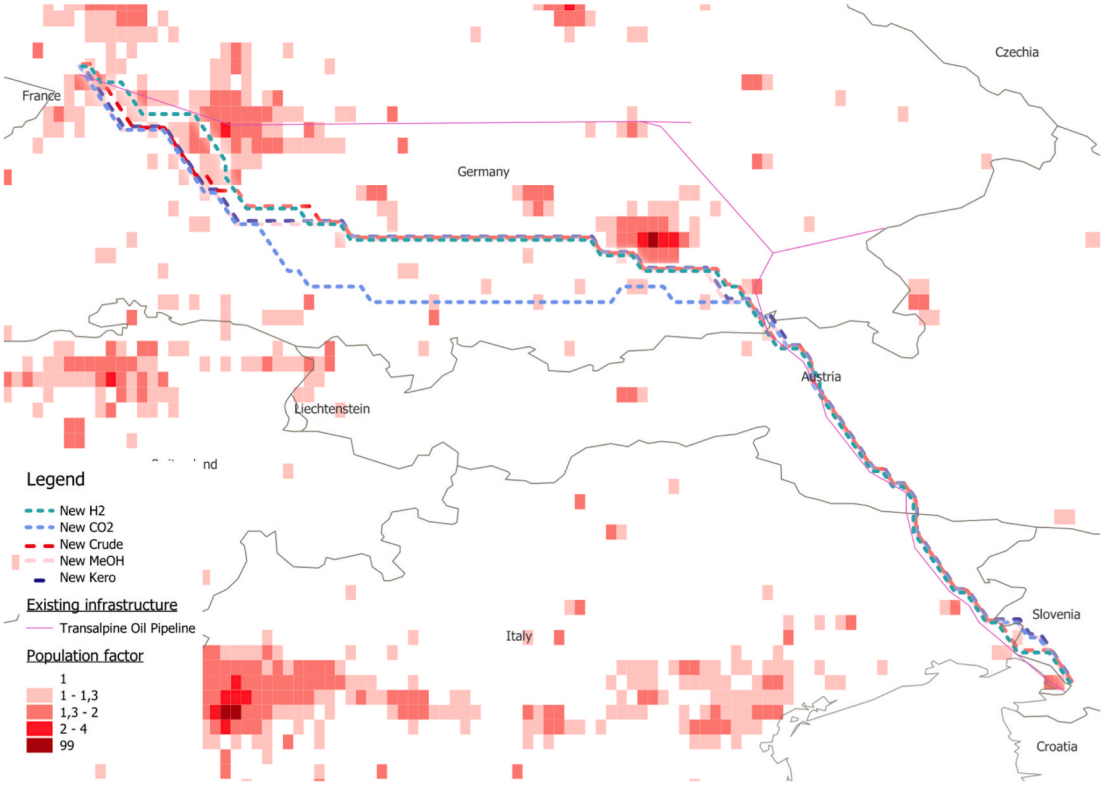


(a) New pipeline configuration

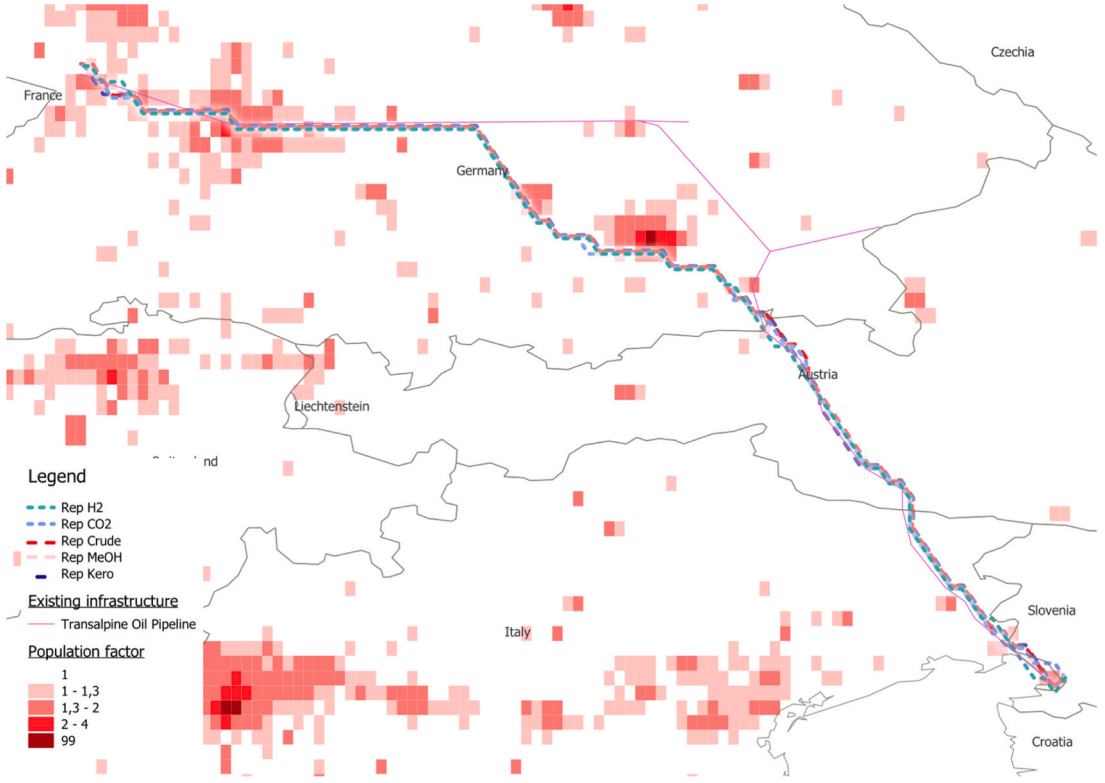


(b) Repurposed pipeline configuration (rep)

Fig. B. 4. Case study - Routing map with slope factors for (a) new and (b) repurposed pipeline configuration.

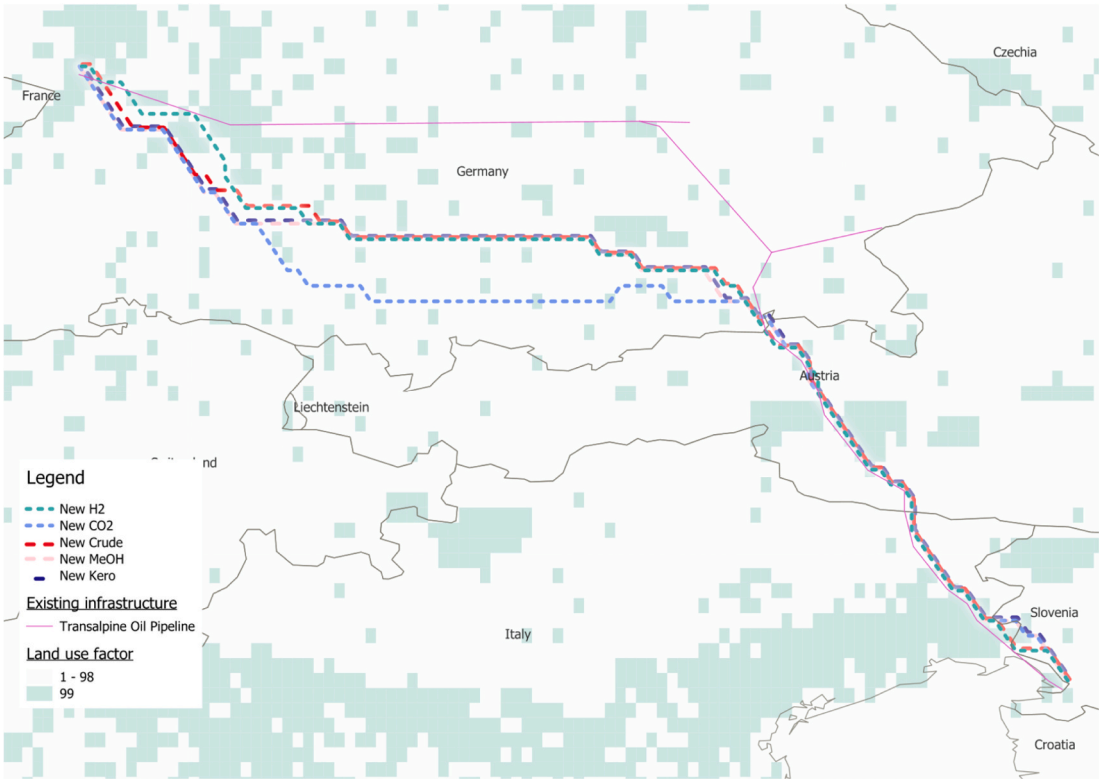


(a) New pipeline configuration

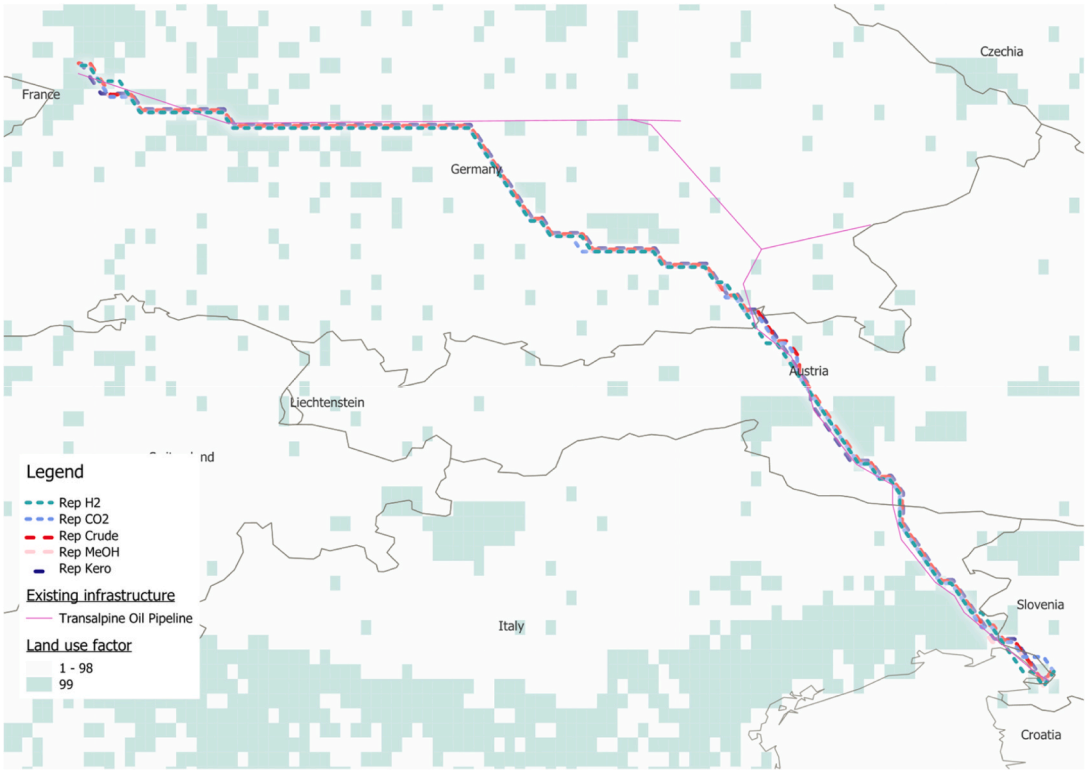


(b) Repurposed pipeline configuration (rep)

Fig. B. 5. Case study - Routing map with population factors for (a) new and (b) repurposed pipeline configuration.



(a) New pipeline configuration



(b) Repurposed pipeline configuration (rep)

Fig. B. 6. Case study - Routing map with land use factors for (a) new and (b) repurposed pipeline configuration.

Data availability

Data will be made available on request.

References

[1] S.J. Davis, et al., Net-zero Emissions Energy Systems, American Association for the Advancement of Science, 29 Jun., 2018. https://www.science.org/doi/10.1126/science.aas9793. (Accessed 29 January 2026).

[2] BMWK, Langfristszenarien: Dashboards [Online]. Available: https://langfristszenarien.de/enertile-explorer-de/. (Accessed 28 August 2025).

[3] G. Luderer, et al., Die Energiewende kosteneffizient gestalten: Szenarien zur Klimaneutralität 2045, Potsdam Institute for Climate Impact Research, 2025 [Online]. Available: https://publications.pik-potsdam.de/pubman/faces/ViewItemOverviewPage.jsp?itemId=item_32090.

[4] K. Machaj, et al., Ammonia as a potential marine fuel: A review, Energy Strategy Rev. 44 (2022) 100926, https://doi.org/10.1016/j.esr.2022.100926.

[5] REGULATION (EU) 2023/1805 OF THE EUROPEAN PARLIAMENT AND OF THE COUNCIL of 13 September 2023 on the use of renewable and low-carbon fuels in maritime transport, and amending Directive 2009/16/EC (Text with EEA relevance), in: Official Journal of the European Union, 2023 [Online]. Available: https://eur-lex.europa.eu/legal-content/DE/ALL/?uri=CELEX:32023R1805. (Accessed 29 January 2026).

[6] Khaled Al-Dabbas, Andreas Clement, Grégoire de Jerphanion, Joshua Fragoso García, Stefan Lechtenböhmer, et al., The impact of EU net-zero industry strategies on the energy system and cross-border hydrogen infrastructure, Energy Strategy Reviews 64 (2026) 102002, https://doi.org/10.1016/j.esr.2025.102002. https://linkinghub.elsevier.com/retrieve/pii/S2211467X25003657.

[7] N. Pieton, M. Neuwirth, M. Jahn, M. Ragwitz, Policy Paper zur Sicherstellung einer mittel- bis langfristigen klimaneutralen Rohstoffversorgung der Raffinerie Schwedt, 2022, https://doi.org/10.24406/PUBLICA-478 [Online]. Available:.

[8] REGULATION (EU) 2023/2405 OF THE EUROPEAN PARLIAMENT AND OF THE COUNCIL of 18 October 2023 on ensuring a level playing field for sustainable air transport (ReFuelEU Aviation) (Text with EEA relevance), in: Official Journal of the European Union, 2023 [Online]. Available: http://data.europa.eu/eli/reg/2023/2405/oj. (Accessed 20 January 2026).

[9] R. Quitzow, A. Nunez, A. Marian, Positioning Germany in an international hydrogen economy: A policy review, Energy Strategy Rev. 53 (2024) 101361, https://doi.org/10.1016/j.esr.2024.101361.

[10] P.C. Verpoort, L. Gast, A. Hofmann, F. Ueckerdt, Impact of global heterogeneity of renewable energy supply on heavy industrial production and green value chains, Nat. Energy 9 (4) (2024) 491–503, https://doi.org/10.1038/s41560-024-01492-z (in En;en).

[11] C. Trompoukis, et al., The role of direct air capture technologies in the EU's decarbonisation effort: Publication for the Committee on industry, research and energy, Luxembourg (Jun. 2025) [Online]. Available: http://www.europarl.europa.eu/supporting-analyses. (Accessed 10 January 2026).

[12] C. Breyer, M. Fasihi, C. Bajamundi, F. Creutzig, Direct air capture of CO2: A key technology for Ambitious climate change Mitigation, Joule 3 (9) (2019) 2053–2057, https://doi.org/10.1016/j.joule.2019.08.010.

[13] BMWK, Importstrategie für Wasserstoff und Wasserstoffderivate [Online]. Available: https://www.bmwk.de/Redaktion/DE/Publikationen/Energie/importstrategie-wasserstoff.pdf?_blob=publicationFile&v=12, 2024.

[14] M. Wietschel, et al., Final Report: HYPAT, Karlsruhe, 2024. https://hypat.de/hypat-en/publications.php. (Accessed 10 March 2025).

[15] IEA, Global hydrogen review 2023, Paris, https://www.iea.org/reports/global-hydrogen-review-2023, 2023.

[16] N. Pieton, et al., In-depth techno-economic assessment of hydrogen and PtX export supply chains: HYPAT, Cottbus, HYPAT working document (2024) [Online]. Available: https://hypat.de/hypat-en/publications.php.

[17] L. Li, P.V. Aravind, A. Boldrini, M. van den Broek, Techno-economic assessment of off-grid hydrogen supply from distant solar or wind sources to steelmaking, Appl. Energy 391 (2025) 125947, https://doi.org/10.1016/j.apenergy.2025.125947.

[18] A.K. Sleiti, W.A. Al-Ammari, L. Vesely, J.S. Kapat, Carbon dioxide transport pipeline systems: overview of technical characteristics, safety, integrity and cost, and potential application of digital twin, J. Energy Resour. Technol. 144 (9) (2022), https://doi.org/10.1115/1.4053348.

[19] Y. Chang, S. Gao, Q. Ma, Y. Wei, G. Li, Techno-economic analysis of carbon capture and utilization technologies and implications for China, Renew. Sustain. Energy Rev. 199 (2024) 114550, https://doi.org/10.1016/j.rser.2024.114550.

[20] D.D. Papadias, J.-K. Peng, R.K. Ahluwalia, Hydrogen carriers: production, transmission, decomposition, and storage, Int. J. Hydrogen Energy 46 (47) (2021) 24169–24189, https://doi.org/10.1016/j.ijhydene.2021.05.002.

[21] Y. Liu, et al., Comprehensive analysis of environmental impacts and energy consumption of biomass-to-methanol and coal-to-methanol via life cycle assessment, Energy 204 (2020) 117961, https://doi.org/10.1016/j.energy.2020.117961.

[22] e.V. Mineralölwirtschaftsverband, Mineralölversorgung mit Pipelines, Feb. 2021. Berlin, https://en2x.de/wp-content/uploads/2022/09/MWV_PIPELINE_Broschu%CC%88re.pdf.

[23] M. Wietschel, et al., Importing hydrogen and hydrogen derivatives: from costs to prices.: HYPAT,, Karlsruhe, HYPAT Working Paper 1/2021 (2021) [Online]. Available: https://hypat.de/hypat-en/publications.php. (Accessed 7 January 2026).

[24] J. Hampp, M. Düren, T. Brown, Import options for chemical energy carriers from renewable sources to Germany, PLoS One 18 (2) (2023) e0262340, https://doi.org/10.1371/journal.pone.0281380.

[25] M. Sterner, et al., 19 Import options for green hydrogen and derivatives - an overview of efficiencies and technology readiness levels, Int. J. Hydrogen Energy 90 (2024) 1112–1127, https://doi.org/10.1016/j.ijhydene.2024.10.045.

[26] A. Taghavi, T. Niknam, S. Shojaeiyan, J. Rodriguez, The future of hydrogen as a strategic enabler in integrated energy systems: Technological developments, barriers, and policy implications, Energy Strategy Rev. 63 (2026) 101999, https://doi.org/10.1016/j.esr.2025.101999.

[27] F. Scheffler, C. Imdahl, S. Zellmer, C. Herrmann, Techno-economic and environmental assessment of renewable hydrogen import routes from overseas in 2030, Appl. Energy 380 (2025) 125073, https://doi.org/10.1016/j.apenergy.2024.125073.

[28] N. Pieton, Transporting the Future: Meta Analysis on Hydrogen, CO2 and Derivatives Transport Costs (In Submission), 2026.

[29] D. DeSantis, B.D. James, C. Houchins, G. Saur, M. Lyubovsky, Cost of long-distance energy transmission by different carriers, iScience 24 (12) (2021) 103495, https://doi.org/10.1016/j.isci.2021.103495.

[30] IEA, World Energy Outlook 2024, IEA Publications, 2024 [Online]. Available: https://iea.blob.core.windows.net/assets/140a0470-5b90-4922-a0e9-838b3ac6918c/WorldEnergyOutlook2024.pdf.

[31] M. Metwally, J. Modisette, Chapter 1: what is a pipeline? in: A. Hoffman, J. Zhang (Eds.), The Atmos Book of Pipeline Simulation, Atmos International, 2022.

[32] M.S. Khairuddin, Effect of elevation to the gas and oil pipeline focusing on pressure drop by using nodal analysis, Bachelor thesis, Universiti Teknologi Petronas (2012) [Online]. Available: https://utpedia.utp.edu.my/id/eprint/3366/.

[33] A.S.M.E. Press (Ed.), Pipeline Pumping and Compression Systems: A Practical Approach, 2008 [Online]. Available:.

[34] E.C. Marcoulaki, I.A. Papazoglou, N. Pixopoulou, An integrated approach to optimal pipeline routing, design, operation and maintenance, in: 21st European Symposium on Computer Aided Process Engineering - ESCAPE 21, 2011, pp. 1753–1757 [Online]. Available: https://www.sciencedirect.com/science/article/pii/B978044454298450129X.

[35] E.C. Marcoulaki, A.V. Tsoutsias, I.A. Papazoglou, Design of optimal pipeline systems using internal corrosion models and GIS tools, Ind. Eng. Chem. Res. 53 (29) (2014) 11755–11765, https://doi.org/10.1021/ie500883g.

[36] B. Weißenburger, L. Karkossa, A. Stephan, R. McKenna, Location matters: Exploring the effects of regional geographical and political characteristics on hydrogen pipeline costs globally [Online]. Available: http://arxiv.org/pdf/2505.01124, May. 2025.

[37] K. Franke, F. Sensfuß, G. Deac, C. Kleinschmitt, M. Ragwitz, Factors affecting the calculation of wind power potentials: a case study of China, Renew. Sustain. Energy Rev. 149 (2021) 111351, https://doi.org/10.1016/j.rser.2021.111351.

[38] S. Raj, V.K. Bansal, "Use of GIS for selection of optimal route for water pipelines in hill areas," (in En;en), Innov. Infrastruct. Solut. 9 (1) (2024) 1–13, https://doi.org/10.1007/s41062-023-01306-3.

[39] T.H. Cormen, C.E. Leiserson, R.L. Rivest, C. Stein, Introduction to Algorithms, third ed., MIT Press, Cambridge, Mass, 2009.

[40] Guidehouse, Five hydrogen supply corridors for Europe in 2030 [Online]. Available: https://ehb.eu/files/downloads/EHB-Supply-corridor-presentation-Full-version.pdf, May. 2022.

[41] TAL Group, Transalpine pipeline route [Online]. Available: https://www.tal-oil.com/en/transalpine-pipeline/route. (Accessed 22 September 2025).

[42] A. Damodaran, Country Risk: Determinants, Measures and Implications – the 2019 Edition, 2019.

[43] Global Energy Monitor, Global gas infrastructure tracker [Online]. Available: https://globalenergymonitor.org/projects/global-gas-infrastructure-tracker/.

[44] Global Energy Monitor, Global oil infrastructure tracker [Online]. Available: https://globalenergymonitor.org/projects/global-oil-infrastructure-tracker/.

[45] T. Galimova, M. Fasihi, D. Bogdanov, G. Lopez, C. Breyer, Analysis of green e-methanol supply costs: domestic production in Europe versus imports via pipeline and sea shipping, Renew. Energy 241 (2025) 122336, https://doi.org/10.1016/j.renene.2024.122336.

[46] J.I. Levene, H2A Hydrogen Delivery Infrastructure Analysis Models and Conventional Pathway Options Analysis Results, Argonne National Laboratory, 2008 [Online]. Available: https://www1.eere.energy.gov/hydrogenandfuelcells/pdfs/nexant_h2a.pdf.

[47] L. Genge, F. Scheller, F. Müsgens, Supply costs of green chemical energy carriers at the European border: a meta-analysis, Int. J. Hydrogen Energy (2023), https://doi.org/10.1016/j.ijhydene.2023.06.180.

[48] NIST, NIST Chemistry WebBook: Standard Reference Database, vol. 69, 2025 [Online]. Available: https://webbook.nist.gov/chemistry/. (Accessed 13 June 2025).

[49] G. Meyer, Thermische Eigenschaften von Mikrokristallinen- und Fischer-Tropsch-Wachsen fraktioniert mit der Kurzweg-Destillation, SOFW-Jurnal, 2012, pp. 58–70, no. 138.

[50] M. Knoope, W. Guijt, A. Ramírez, A. Faaij, Improved cost models for optimizing CO2 pipeline configuration for point-to-point pipelines and simple networks, Int. J. Greenh. Gas Control 22 (2014) 25–46, https://doi.org/10.1016/j.ijggc.2013.12.016.

[51] Mineralölverbundleitung GmbH Schwedt, Technische details [Online]. Available: https://www.mvl-schwedt.de/ueber-uns/unternehmen/technische-details. (Accessed 20 August 2024).

[52] M.A. Khan, C. Young, C. MacKinnon, D. Layzell, The techno-economics of hydrogen compression, Transition Accelerator Technical Briefs (1) (2021) 1–36

[Online]. Available: https://transitionaccelerator.ca/wp-content/uploads/2023/04/TA-Technical-Brief-1.1_TEEA-Hydrogen-Compression_PUBLISHED.pdf.
[53] S. Kaiser, F. Siems, C. Mostert, S. Bringezu, Environmental and economic performance of CO2-based methanol production using long-distance transport for H2 in combination with CO2 point sources: a case study for Germany, Energies 15 (7) (2022) 2507, https://doi.org/10.3390/en15072507.
[54] M. Niermann, S. Timmerberg, S. Drünert, M. Kaltschmitt, Liquid Organic Hydrogen Carriers and alternatives for international transport of renewable hydrogen, Renew. Sustain. Energy Rev. 135 (2021) 110171, https://doi.org/10.1016/j.rser.2020.110171.
[55] Bundesnetzagentur, Wasserstoff-kernnetz: Geänderte Anlage 4: Neubaumaßnahmen (Antrag 22.07 [Online]. Available: https://www.bundesnetzagentur.de/DE/Fachthemen/ElektrizitaetundGas/Wasserstoff/Kernnetz/start.html, 2024. (Accessed 13 March 2025).
[56] Bundesnetzagentur, Wasserstoff-kernnetz: Geänderte Anlage 3: Umstellungsmaßnahmen (Antrag 22.07 [Online]. Available: https://www.bundesnetzagentur.de/DE/Fachthemen/ElektrizitaetundGas/Wasserstoff/Kernnetz/start.html, 2024. (Accessed 13 March 2025).
[57] IEA GHG, Transmission of CO2 & energy, Report Number PH4/6, https://publications.ieaghg.org/docs/General_Docs/Reports/PH4_6%20TRANSMISSION%20REPORT.pdf, Mar. 2002.
[58] A. de Klerk, Environmentally friendly refining: Fischer–Tropsch versus crude oil, Green Chem. 9 (6) (2007) 560–565, https://doi.org/10.1039/B614187K.
[59] Engineering ToolBox [online]. [Online]. Available: https://www.engineeringtoolbox.com/. (Accessed 14 June 2025).
[60] G. Towler, R. Sinnot, Chemical Engineering Design: Principles, Practice and Economics of Plant and Process Design, Elsevier, USA, 2007 [Online]. Available: https://nitsri.ac.in/Department/Chemical%20Engineering/PED_ResourceBook1.pdf. (Accessed 18 July 2024).
[61] M. Metwally, J. Modisette, Chapter 7: pipeline and compression, in: A. Hoffman, J. Zhang (Eds.), The Atmos Book of Pipeline Simulation, Atmos International, 2022, pp. 214–278.
[62] H2tools, Hydrogen Compressibility at different temperatures and pressures [Online]. Available: https://h2tools.org/hyarc/hydrogen-data/hydrogen-compressibility-different-temperatures-and-pressures. (Accessed 15 January 2025).
[63] D. Morgan, A. Guinan, A. Sheriff, FECM/NETL CO2 transport cost model: description and user's manual, Pittsburgh, DOE/NETL 2022/3218 (2022) [Online]. Available: https://netl.doe.gov/projects/files/FECMNETLCO2TransportCostModel2024DescriptionandUsersManual_082324.pdf. (Accessed 31 January 2026).
[64] E.C. Marcoulaki, I.A. Papazoglou, N. Pixopoulou, Integrated framework for the design of pipeline systems using stochastic optimisation and GIS tools, Chem. Eng. Res. Des. 90 (12) (2012) 2209–2222, https://doi.org/10.1016/j.cherd.2012.05.012.
[65] F. Staiß, M. Schmdit, C. Stephanos, P. Stöcker, S. Wurbs, Optionen für den Import grünen Wasserstoffs nach Deutschland bis zum Jahr 2030 [Online]. Available: https://energiesysteme-zukunft.de/publikationen/materialien/transportoptionen-wasserstoff-2030, Nov. 2022. (Accessed 17 September 2023).
[66] FNB Gas, Netzentwicklungsplan gas 2020-2030 [Online]. Available: https://fnb-gas.de/wp-content/uploads/2021/09/fnb_gas_nep_gas_2020_de-1.pdf, 2021. (Accessed 15 June 2025).
[67] The U.S. Department of Transportation, Transport of Methanol by Pipeline, 1985. Washington, D.C.. (Accessed 31 January 2026).
[68] D.R. Woods, Appendix D: capital cost guidelines, in: Rules of Thumb in Engineering Practice, John Wiley & Sons, Ltd, 2007, pp. 376–436 [Online]. Available: https://onlinelibrary.wiley.com/doi/10.1002/9783527611119.app4.
[69] A. Almasi, "Estimate Pump Installation Costs," *Pumps & Systems*, 2014. https://www.pumpsandsystems.com/estimate-pump-installation-costs. (Accessed 4 January 2025).
[70] M.D. Solomon, M. Scheffler, W. Heineken, M. Ashkavand, T. Birth-Reichert, Pipeline infrastructure for CO2 transport: cost analysis and design optimization, Energies 17 (12) (2024) 2911, https://doi.org/10.3390/en17122911.
[71] M. Moritz, M. Schönfisch, S. Schulte, Estimating global production and supply costs for green hydrogen and hydrogen-based green energy commodities, Int. J. Hydrogen Energy 48 (25) (2023) 9139–9154, https://doi.org/10.1016/j.ijhydene.2022.12.046.
[72] R.S. Aries, R.D. Newton, Chemical engineering cost estimation [Online]. Available: https://search.worldcat.org/de/title/576484307. (Accessed 16 July 2024).
[73] C. Weimer, How Old is Too Old? A Look at aging transmission pipeline infrastructure issues [Online]. Available: https://pstrust.org/wp-content/uploads/2015/12/Weimer-Old-Pipes.pdf, 2015.
[74] Hydraulic Institute, Europump, and US Department of Energy's Office of industrial technologies (OIT), "pump life cycle costs: a guide to LCC analysis for pumping systems: Executive summary," [Online]. Available: https://www.energy.gov/eere/amo/articles/pump-life-cycle-costs-guide-lcc-analysis-pumping-systems-executive-summary, 2001. (Accessed 17 July 2024).
[75] C. Yang, J. Ogden, Determining the lowest-cost hydrogen delivery mode, Int. J. Hydrogen Energy 32 (2) (2007) 268–286, https://doi.org/10.1016/j.ijhydene.2006.05.009.
[76] J. Phillip Ellenberger (Ed.), Piping and Pipeline Calculations Manual, second ed., Butterworth-Heinemann, Boston, 2014.
[77] L. Zeghadnia, J.L. Robert, B. Achour, Explicit solutions for turbulent flow friction factor: a review, assessment and approaches classification, Ain Shams Eng. J. 10 (1) (2019) 243–252, https://doi.org/10.1016/j.asej.2018.10.007.
[78] ENTSOG, System capacity map [Online]. Available: https://www.entsog.eu/maps, 2025. (Accessed 10 March 2025).